Journal of Marine Science and Application (2024) 23: 960-983
https://doi.org/10.1007/s11804-024-00444-z

RESEARCH ARTICLE

Energy-Efficient and Reliable Deployment Models for Hybrid Underwater Acoustic Sensor Networks with a Mobile Gateway

Tatiana A. Fedorova[1], Vladimir A. Ryzhov[1], Kirill S. Safronov[1], Nikolay N. Semenov[2] and Shaharin A. Sulaiman[3]

Received: 26 September 2023 / Accepted: 06 January 2024

Abstract

This work proposes an innovative approach to evaluate the functional characteristics of a heterogeneous underwater wireless acoustic sensor network (UWASN) using a stochastic model and the network connectivity criterion. The connectivity criterion is probabilistic and considers inherently distinct groups of parameters: technical parameters that determine the network function at specific levels of the communication stack and physical parameters that describe the environment in the water area. The proposed approach enables researchers to evaluate the network characteristics in terms of energy efficiency and reliability while considering specific network and environmental parameters. Moreover, this approach is a simple and convenient tool for analyzing the effectiveness of protocols in various open systems interconnection model levels. It is possible to assess the potential capabilities of any protocol and include it in the proposed model. This work presents the results of modeling the critical characteristics of heterogeneous three-dimensional UWASNs of different scales consisting of stationary sensors and a wave glider as a mobile gateway, using specific protocols as examples. Several alternative routes for the wave glider are considered to optimize the network's functional capabilities. Optimal trajectories of the wave glider's movement have been determined in terms of ensuring the efficiency and reliability of the hybrid UWASN at various scales. In the context of the problem, an evaluation of different reference node placement was to ensure message transmission to a mobile gateway. The best location of reference nodes has been found.

Keywords Heterogeneous underwater wireless acoustic sensor network; Mobile gateway; Wave glider; Stochastic connectivity model; Probabilistic optimality criteria; Network reliability; Network energy consumption

Article Highlights

- A special stochastic characteristic of the quality of UWASN functioning, connectivity, is proposed, which covers both static and dynamic characteristics of the network, as well as environmental conditions.
- Criteria for reliability and efficiency have been developed based on connectivity, taking into account physical parameters of the environment and technical characteristics of the network.
- Modeling of the critical characteristics of heterogeneous three-dimensional UWASNs, consisting of stationary sensors and a wave glider as a mobile gateway, has been conducted.
- The optimal trajectories for the wave glider's movement and the optimal placement of reference nodes have been determined to ensurethe efficiency and rel iability of the hybrid UWASN at various scales.

✉ Shaharin A. Sulaiman
shaharin@utp.edu.my

[1] Department of Applied Mathematics and Mathematical Modeling, Saint Petersburg State Marine Technical University, Saint Petersburg 190121, Russia

[2] Department of Marine Information Systems and Technologies, Saint Petersburg State Marine Technical University, Saint Petersburg 190121, Russia

[3] Department of Mechanical Engineering, Universiti Teknologi PETRONAS, Seri Iskandar 32610, Malaysia

1 Introduction

One of the most critical areas of research on underwater wireless acoustic sensor network (UWASN) functioning is the evaluation of energy consumption of particular network elements and the entire network as a whole so it can be minimized. Reducing energy consumption allows the network lifespan to increase without recharging the batteries. Thus, energy management is one of the main factors determining the efficient functioning of underwater wireless networks.

In this work, a new stochastic functional quality characteristic of the UWASN is introduced and analyzed. The characteristic, called the probabilistic criterion of network connectivity, reflects the ability of the network to establish reliable connections between sensors. It determines the probability of packet delivery from ordinary sensors through a selected set of reference sensors to a mobile gateway under the given design parameters of the network and the physical conditions of the water area. The packet delivery probability, in turn, is the main parameter of the stochastic model for the UWASN function, previously proposed by Fedorova et al. (2022). The network connectivity criterion considers several distinct groups of parameters, including the following:

1) Main technical characteristics of the transmitting and receiving devices.

2) Parameters connected with the network topology, such as the distribution of sensors in the three-dimensional (3D) space of the water area.

3) Physical characteristics of the medium, such as the signal attenuation coefficient and noise level in the water area.

4) Timing characteristics, such as the time scale and frequency of information collection by the sensors.

In underwater wired sensor networks with a centralized energy source, the reliability (connectivity) of the data transmission depends mainly on the choice of the optimal network topology. Energy efficiency is not of fundamental importance for wired networks. However, when determining the connectivity of underwater wireless sensor networks, not only the chosen topology, network congestion, and sensor reliability must be considered, but also the residual battery energy of each device. This is because connectivity failures can be caused by disruptions in data transmission routes when the battery of any of the sensors is exhausted, the inability to establish a reliable connection due to insufficient signal power to the transmitting antenna of a sensor device, or too great a distance to neighboring sensors while with a significant signal attenuation coefficient in the medium.

The residual battery energy of each sensor determines the current energy state of the entire network. It is a function of energy consumption, which, in turn, depends on the network scale (water area size), network architecture, selected protocols for various levels of network functioning, physical conditions in the water area, and the network purpose (practical application and polling frequency). Changing the network scale or distance between sensors, designing special routing algorithms, as well as changing the technical characteristics of modems can significantly reduce energy consumption. This means that it is possible to recover connectivity that is partially lost during wireless network functioning not only by charging the battery but also by changing the topological or technical parameters of the wireless sensor network, by changing the sensor interaction protocols, or by using mobile sensor platforms.

Connectivity, as a dynamic functional quality characteristic of the underwater wireless sensor network, is a generalized characteristic that indirectly determines the network lifespan. The lifespan is the time from the moment the network is launched until the battery of any of the sensors (or a certain percentage of the sensors) is discharged. Thus, network lifespan can be considered as a special case of connectivity, determined by the loss of connection with one or more network devices.

Changing a few technical parameters, such as transmitting modem power or data transmission speed, rebuilding packet delivery routes to reference nodes, or rerouting mobile gateways, restores the connectivity of network elements without recharging the batteries of failed devices. For example, increasing the transmitting modem's power allows packets to be transmitted to more distant sensors, bypassing the failed ones; concurrently, the mobile gateway (e.g., a wave glider (WG)) rerouting can reduce the energy consumption of the network.

Thus, there are several possibilities to extend the lifespan of the entire network (but not its individual elements) without recharging the sensor batteries. So network connectivity, as opposed to lifespan, characterizes the entire network rather than the properties of its elements.

The object of the study in this work is an UWASN 3D communication architecture, which includes a group of ordinary and reference stationary nodes in three different layers—on the bottom (bottom layer), in the water column (middle layer), and near the surface (upper layer)—as well as a mobile gateway, a wave glider moving on the surface of the water area. Packet transfer between network nodes is conducted by hydroacoustic channel.

The subject of the study is a stochastic connectivity model of an underwater wireless sensor network, including probabilistic criteria of packet transmission reliability and network energy consumption efficiency.

This work proposes a generalized connectivity criterion as the probability of packet delivery, which, in turn, is the main parameter of the stochastic model. This generalized criterion includes probabilistic criteria of network reliability and efficiency. This work investigates their dependence on such network parameters as the scale, the distribution of ordinary and reference nodes within the water area, mobile gateway routes, and routing protocols.

The following probabilistic optimality criteria were selected as UWASN connectivity criteria, determined for a given signal-to-noise ratio (SNR), signal attenuation coefficient in the water area, network scale, and the specific parameters of the physical layer protocol and routing protocol:

1) Probabilistic criterion of reliability—a measure of the probability of successful packet delivery to the mobile gateway.

2) Probabilistic criterion of the efficiency of the network energy consumption.

The latter criterion involves the evaluation of two characteristics:

1) An estimate of the network's relative energy consumption—the ratio of the real energy consumption of the entire network under the chosen routing protocol to the full consumption corresponding to 100% packet delivery for an unlimited number of retransmissions.

2) An estimate of the value of the total expected energy consumption of the network under the given physical conditions in the water area for the selected design parameters.

This work is organized as follows. A brief literature review of related research is given in Section 2. Section 3

describes the communication architecture of the underwater wireless sensor network. Section 4 defines the design parameters for modeling the functional characteristics of the network. Section 5 introduces a generalized probabilistic connectivity criterion of the UWASN. A mathematical model for evaluating the basic functional characteristics of the 3D UWASN is presented in Section 6. Different reference nodes locations were proposed in Section 7. A comparison of reference nodes locations and optimization of network architecture is given in Section 8. The conclusions are presented in Section 9.

2 Related work

Overcoming the problems associated with the features of the underwater acoustic channel determined by its dynamic properties—high signal propagation delay, limited bandwidth, low data transmission rate, and high probability of bit errors—is necessary to develop an effective UWASN (Zorzi et al., 2008; Davis and Chang, 2012). We also consider the fact that UWASNs consume much more energy than terrestrial sensor networks (receive and transmit power ratio 1: 125 (Freitag et al., 2005)) and that the technical components of UWASNs have limited energy resources, for which replenishment is problematic (Rahman et al., 2017). Therefore, energy consumption management in UWASNs is also a big problem that determines the network lifespan. In addition, various practical applications such as oceanographic data collection, pollution monitoring, maritime reconnaissance, navigational safety, or distributed tactical surveillance (Akyildiz et al., 2005; Pompili et al., 2010), impose their specific constraints and requirements on the architecture and design parameters of the developed underwater networks.

One of the main goals of designing an effective UWASN, regardless of application, is to achieve a high packet delivery ratio while limiting the end-to-end delay and the power consumption of the network components (Lu et al., 2017), ensuring high network reliability. Designing a UWASN that meets the criteria of reliability and energy efficiency is obviously a complex and quite difficult problem. The considered optimization problem is multiparameter and multicriteria and requires a comprehensive analysis of the influences of a set of parameters with different natures, both technical and physical, on the main functional characteristics of UWASN. Many studies are devoted to the analysis of the development of reliable and energy-efficient UWASN.

The lifespan of a network with limited battery capacity at the network nodes is determined by its energy efficiency. During its functioning, energy holes/void areas may appear in the network due to some nodes ceasing to work and, thus, decrease the network performance. The causes of void areas are the failure of nodes due to limited lifespan, damaged sensors, sparse network topology, varying hydroacoustic channel characteristics, or the impact of technical objects and marine animals. When a certain fixed number of nodes fail, the network goes down (groups of nodes whose packet delivery routes passed through the failed nodes may be inaccessible). The energy efficiency of the network depends on many physical and technical parameters of the medium, the network architecture, and the technical parameters of the receiving and transmitting devices. Correct accounting for and selection of these parameters reduces the negative impact of void areas and lack of power for data transmission. The problem of eliminating energy holes/void areas in UWASN can be solved by various methods (Azam et al., 2016; Chaaf et al., 2021; Khan et al., 2021; Mhemed et al., 2022).

There are many works devoted to the improvement of the UWASN energy efficiency. As a rule, these works consider the effect of a limited number of design parameters (one or more) on energy efficiency while maintaining the required reliability of operation. Specific examples are aimed at the following approaches:

1) Improving the technical parameters of power sources and the economics of modems (Tokmachev et al., 2021; Chen et al., 2022; Sherlock et al., 2022; Li et al., 2022).

2) Controlling network topology (Datta and Dasgupta, 2023; Sutagundar et al., 2022; Choudhary and Goyal, 2022).

3) Using mobile nodes (Datta and Dasgupta, 2023; Choudhary and Goyal, 2022; Hu et al., 2022; Fedorova et al., 2022).

4) Developing energy-efficient routing protocols (Ahmad et al., 2022; Bharany et al., 2023; Sheeja et al., 2023; Alfajeer and Harous, 2022; Shovon and Shin, 2022; Hao et al., 2021; Chen et al., 2010; Kampen, 2021; Isufi et al., 2016; Touzen, 2020; Ali et al., 2014; Ahmed et al., 2017; Menon and Prathap, 2016; Hyder et al., 2017; Jiang, 2018; Aljughaiman et al., 2020; Tiwari and Singh, 2023; Vijay et al., 2023).

5) Developing effective medium access protocols (Guqhaiman et al., 2020; Kulla et al., 2022; Gazi et al., 2022; Liu et al., 2021; Lu and Shengming, 2016; Hyder et al., 2017; Jiang, 2018; Aljughaiman et al., 2020; Khan et al., 2022; Tang et al., 2023).

6) Optimizing data communication protocols (e. g., data link protocols) and packet sizes (Kebkal et al., 2005; Stojanovic, 2005; Shahapur and Khanai, 2015; Di Valerio et al., 2015; Xu et al., 2022; Heidemann et al., 2012; Yigit et al., 2018; Yildiz et al., 2018; Basagni et al., 2012; Kebkal et al., 2019; Jung and Abdullah, 2011; Khan et al., 2022).

7) Modernizing physical layer protocols (e. g., methods of signal formation and processing) and improving modem technical parameters (Shahapur and Khanai, 2015; Songzuo et al., 2021; Casari et al., 2022; Goyal et al., 2019; Scussel et al., 1997; Cao et al., 2018; Bernard et al., 2022; Wang et al., 2022; Pan et al., 2018; Schmidt et al., 2019;

Jiang et al., 2022; He et al., 2017; Mani et al., 2008).

The work proposed here is related to both network topology control and the use of mobile nodes to enhance the efficiency of UWASN operation. Therefore, we briefly explore the research conducted previously in these areas.

As noted previously, energy holes/void areas can appear in the network topology during UWASN functioning. Thus, some network nodes may not be available for operation, and the connectivity and coverage of the entire network cannot be guaranteed. To solve this problem, an efficient UWASN topology control/management algorithm is important (Datta and Dasgupta, 2023; Sutagundar et al., 2022; Choudhary and Groyal, 2022). Topology control is subdivided into topology construction and topology maintenance. These processes are important for building efficient solutions that save energy and, as a result, prolong the network lifespan.

Construction of the initial network topology (network deployment) has been considered in detail (Liu et al., 2019; Sharma and Bindal, 2014; Arivudainambi et al., 2017; Choudhary and Goyal, 2021; Chaudhary et al., 2022; Fattah et al., 2022). Types of network deployment studied included static deployment, self-adjusting deployment, and movement-assisted deployment. Models were built of networks using different sensor types and forming clustered and nonclustered topologies. The deployment objectives were to reduce the overlapping problem, optimize gateway deployment, increase the network lifespan, maintain the network connectivity, minimize the uncovered area, maximize the coverage and connectivity, drive the autonomous underwater vehicle to the target, or minimize the distance and travel time.

The main goal of topology control is to improve both the energy efficiency of the UWASN and to provide a guaranteed quality of service (QoS) (Hong et al., 2018).

Works on network topology control used different methods and algorithms (e. g., Liu et al., 2019; Sharma and Bindal, 2014; Arivudainambi et al., 2017; Choudhary et al., 2021; Chaudhary et al., 2022; Fattah et al., 2022). In many studies of the UWASN topology control algorithms, network connectivity and coverage were considered the main network evaluation criteria (Coutinho et al., 2018). In the topology control algorithm (Hefeeda and Ahmadi, 2007), the data packet transmission rate has been used to determine node connectivity. Tan and Wu (2004) introduced the concept of network structure entropy and node connectivity with network structure entropy, connectivity, and coverage adopted as network functioning evaluation indices, which reflected the topology reliability. In Yang et al. (2015), the network topology control algorithm was based on game theory, which equalized the energy consumption of the nodes. Liu et al. (2014) proposed a 3D underwater fault-tolerant topology to improve network reliability by maintaining K-connectivity, but their algorithm did not consider node degree, channel redundancy, propagation delay, etc. The proposed network topology control algorithm was based on the potential game and optimal rigid subgraph to eliminate redundant links in the network topology and reduce the load on the nodes. Thus, it follows from the analysis of works on this topic that network deployment end management is multiparametric and multifunctional and is aimed at improving the energy efficiency and reliability of the network.

The current study explores options for constructing a UWASN topology that considers both the technical parameters of devices and the physical parameters of the environment. The aim is to ensure sufficiently high energy efficiency in the UWASN while maintaining guaranteed throughput, network connectivity, and coverage.

The use of a mobile sink is remarkably effective in a UWASN. Mobile sinks combat energy holes/void areas, ensuring timely data collection from network nodes and reducing the number of packet retransmissions from end nodes to the mobile gateway. Variable network topology increases the energy efficiency and reliability of the entire network if some nodes are out of service. Various underwater and surface robotic platforms can function as mobile sinks (Choudhary and Goyal, 2022; Hu et al., 2022; Fedorova et al., 2022; Lan et al., 2021; Li et al., 2022; Ovchinnikov et al., 2020; Nam, 2018; Jawhar et al., 2019; Cai and Zhang, 2016). Underwater mobile platforms include autonomous unmanned vehicles, underwater gliders, and radio-hydroacoustic moored buoys; surface platforms include crewless boats and platforms propelled by renewable solar, wind, and sea energy, such as wave gliders. The advantage of using wave gliders as a mobile sink, compared to the other platforms, is the combination of such functional characteristics as high autonomy, high power capacity, and the ability to function as a gateway for intermediate data transfer (Fedorova et al., 2022; Lan et al., 2021; Li et al., 2022). Wave gliders also have a disadvantage: limited velocity and, therefore, low stability under external disturbances. Despite this drawback, the wave glider is a suitable candidate as a mobile sink for many practical applications.

The number of publications related to the use of a WG as a mobile gateway is small. Therefore, in a continuation of previous work (Fedorova et al., 2022), the authors of this study further explore the potential of a WG for UWASNs of various scales.

Another crucial metric for the UWASN is reliability. The reliability and energy efficiency of the network are closely related. The main characteristics of network reliability are the packet delivery ratio (PDR) and the end-to-end delay. These characteristics define the QoS from the point of view of the user of a particular application.

The packet delivery probability is defined as the ratio of the number of packets that successfully reach the surface receiver to the number of packets transmitted by the source.

Studies also use the probability of packet loss, which is inversely proportional to the PDR. The end-to-end packet delivery delay is defined as the average transmission delay between the source and the surface receiver.

The packet delivery probability is related to the network topology; that is, the number of sensor nodes and their distribution density in the water area, the routing protocol used, the network load, the use of mobile gateways in the network, the signal attenuation coefficient, the transmitter power, the receiver sensitivity, and the ambient noise.

Studies have shown (Shental et al., 2005; Khasawneh et al., 2020; Rajeswari et al., 2020; Venkateswara and Malladi, 2021) that the value of the PDR increases with the density of network nodes for most routing protocols. This is because the higher the number of nodes in the network, the higher the probability of selecting the next forwarding node. Thus, the probability of packet loss due to node unavailability within the forwarding zone is reduced. Simultaneously, the average end-to-end packet delivery delay decreases.

Efficient routing protocol algorithms are designed to attain the best PDR while limiting energy consumption and end-to-end delay. Therefore, different routing protocols have different PDRs.

Attaining high PDR values for an effective routing protocol is related to the problem of reducing the negative effect of energy holes/void areas. Studies of the effect on the PDR of different numbers of void areas in the water area with a fixed number of nodes showed that the PDR increases with increasing node density in the water area with the same number of void areas for effective routing protocols.

The PDR is also related to network load (Shental et al., 2005). As a rule, with an increase in network load (the number of packets forwarded per unit time), the number of lost packets increases, which decreases the PDR. Therefore, routing protocols under development are aimed at improving functioning related to increasing network bandwidth and reducing long end-to-end delays.

It follows from this brief overview that the range of research areas related to the development of an energy-efficient and reliable underwater hydroacoustic network is broad. The studies show that the problem to be solved is multiparameter and multicriteria, and the simultaneous consideration of many interrelated parameters, constraints, and requirements is problematic. We cannot discuss optimal network development in a global sense yet, because this requires building a complicated mathematical/simulation model hierarchy that is adaptive to real dynamically changing medium characteristics and that operates with big data (Rahman et al., 2023; Wang et al., 2017; Jahanbakht et al., 2021).

An alternative approach to a comprehensive analysis can be proposed, which consists of a simple stochastic model of UWASN functioning evaluation, using a generalized system that combines the different parameters relating to the processes of the lower levels of the OSI. Such a system allows us to conduct an engineering analysis of network functional characteristics in terms of the connectivity of the system. The term connectivity was introduced for terrestrial wireless networks. For underwater applications, this term was used in relation to optical sensor networks, where coherence was understood as a geometric characteristic determining the line-of-sight location of two nodes, as well as in relation to underwater network topology control (Datta and Dasgupta, 2023; Sutagundar et al., 2022; Choudhary and Goyal, 2022; Li et al., 2022; Sharma and Bindal, 2014; Arivudainambi et al., 2017; Choudhary and Goyal, 2021; Chaudhary et al., 2022; Fattah et al., 2022; Hong et al., 2018; Coutinho et al., 2018; Hefeeda and Ahmadi, 2007; Tan and Wu, 2004; Yang et al., 2015; Liu et al., 2014). In the context of this work, connectivity is defined as a stochastic functional characteristic of UWASN, reflecting the ability of the network to establish reliable communication between all network components. The influence of several technical and physical parameters on ensuring network connectivity is investigated using this approach in this work.

In contrast to the reviewed works, the authors propose the following innovative approaches to solving the problem of constructing an optimal hybrid UWASN:

1) A parametric probabilistic model that allows for qualitative and quantitative assessments of the functional characteristics of the UWASN in analytical form.

2) Basic trajectory options for a mobile gateway, based on which an analytical prediction of the most suitable trajectory at the considered network scale is made. These data can serve as initial approximations for numerical models to refine the optimal solution.

3) A new connectivity criterion, which is a generalized characteristic including the probabilistic criteria of network reliability and efficiency. This criterion indirectly determines the network lifespan.

3 3D communication architecture of a UWASN

This section presents the 3D communication architecture of a UWASN, introduces the main notations, and gives the simplifying assumptions. Four methods for deploying reference nodes in the water area are selected and justified.

It is assumed that the UWASN is in the water area in a physically heterogeneous medium and has the form of a 3D orthogonal lattice (Figure 1). We assume that the 2D levels in the 3D lattice located near the surface, in the water column, and near the bottom are parallel and in layers of the medium that are homogeneous in terms of temperature, density, salinity, and turbidity. Therefore, each layer is characterized by its signal attenuation coefficient (Figure 1).

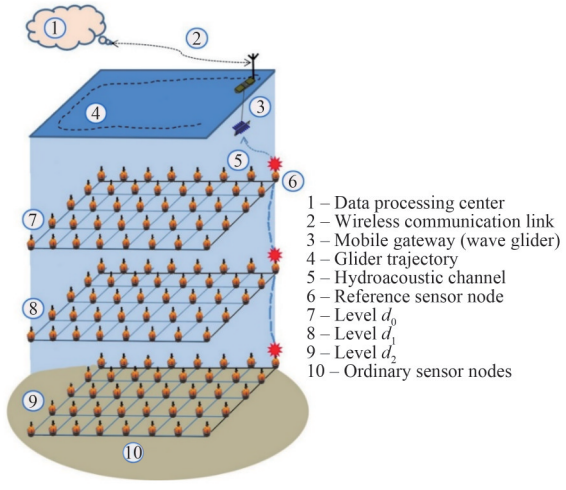

Figure 1 3D underwater wireless acoustic sensor network model with a single mobile gateway (wave glider) for an arbitrary $n \times n \times 3$ network dimension

In each layer there are several reference nodes deployed in a certain way. Information from ordinary nodes is transmitted to the nearest reference node. Ordinary sensors measure some set of physical parameters of the medium, process this data, and transmit this information directly or through a set of neighbors to the nearest reference node. Ordinary sensors first transmit packets to the reference sensors of their layer, and then the reference sensors transmit packets vertically upward to the reference sensors of the upper layers. Due to the peculiarities of signal propagation in the marine layered medium (the vertical distribution of temperature along the depth is uneven; therefore, the speed of sound along the depth is also uneven), the direction of signal propagation curves toward the layer with a lower sound speed. Therefore, zones of signal absence or attenuation appear. The vertical distribution of sound velocity varies with the time of year and the current weather; therefore, it is difficult to predict the quality of hydroacoustic communication. The proposed model assumes that signal transmission is strictly vertical because when the signal propagates along the normal to the horizontal layers with the same sound velocity, there is no curvature of the signal propagation direction, and the packet delivery does not depend on the vertical sound velocity distribution by depth (Ahmed and Younis, 2019).

It is assumed that the network functioning time between two measurements is equal to T (cycle time). During this time, all measurement results must be delivered to the WG mobile gateway.

The cycle time can be different for different applications and ranges from a few minutes to hours or even days. In addition, T must correlate with the technical (speed) capabilities of the WG mobile agent of the network. Therefore, the cycle time is supposed to be such that the WG has time to traverse across all the reference nodes located in the water area of the given size during this time. Certainly, the WG speed characteristics impose strict restrictions on the size of the serviced water area and on the satisfaction of the cyclic data acquisition requirements. Therefore, more than one mobile agent may be required for an effective solution to the applied problem. In this work, we consider the base case of a single mobile agent servicing the water area during the time interval T.

Each of the sensor subsystems—data acquisition, processing, and transmission—needs energy from an electric battery, but the main consumer is a transmitting modem, which needs approximately a million times more energy to transfer one bit of data than is needed to collect or process one bit in the microcontroller. So, accurate evaluation of the connectivity of an underwater wireless sensor network is determined by estimating the energy consumed by the sensor to send packets according to the selected network protocols.

Consider a wireless sensor network in which all sensors are divided into clusters based on proximity to a particular reference node. Each cluster contains one reference node and several ordinary nodes. The most general case of such an architecture is a wireless sensor network, in which any sensor in a cluster can function as a reference node at different points in time. Such a network is efficient and scalable, provided that the reference node is chosen rationally at a particular point in time. Examples of reference node selection protocols are the well-known low-energy adaptive clustering hierarchy (LEACH) or base-station controlled dynamic clustering protocol (BCDCP) (Heinzelman et al., 2002; Vhatkar et al., 2015), which rely on selecting the device with the highest residual energy level. Suppose that each of the devices generates packets with some periodicity and transmits them to a reference node. There are two variants of data transmission within the cluster: direct transmission of packets from each sensor directly to the reference node without transits or transit transmission using some sensors of the same cluster as intermediate ones.

A sensor can lose the ability to transmit data to a reference node at any time for many reasons: external influences, hardware failure, software failures, etc. However, one event inevitably leads to node failure—the discharge of the sensor node battery. Obviously, the occurrence of this event depends on the initial capacity of the battery and the total energy consumption during the functioning of the node. The energy consumption, in turn, is a random variable that is influenced by the following parameters of the UWASN:

1) Amount of data transmitted, related to the scale of the network and the total number of sensors n^2.

2) Modem power P_s.

3) Selected carrier frequency f and data bit rate f_{bit}.

4) Cluster scale related to the number of reference nodes m.

5) Number of hops (transits) during packet transmission.

6) Distribution of sensor devices in space—the depth of layers from the surface h_i and the density of sensor devices,

in our case, it is the distance between sensors on the horizontal level r.

7) Routing protocols and their characteristics—in the present work, we vary the number N of allowed retransmissions of one packet between neighbors.

8) Parameters related to the physical characteristics of the medium, such as the signal attenuation coefficient β and the noise level in the water area SNR.

Not all attempts to transmit a packet from a sensor node to a neighbor can be successful. Assuming the possibility of multiple transmission attempts at intervals, the packet delivery from the sensor device to the reference node will be a random variable that depends on the connectivity probability of the network. Assume that after a fixed number of transmissions N no packet is delivered to the nearest neighbors, the packet is considered lost, and the sensor proceeds to forward the next packet standing in the queue.

The division of the sensor network into clusters is primarily determined by the optimal location of the reference nodes because all information from the ordinary nodes flows to them. Obviously, the bandwidth of the reference node is limited, and if the network is large and the reference node location is poor, bottlenecks may appear, where the energy consumption increases sharply, leading to rapid battery discharge. To prevent this, in this work, we investigate several options for the location of reference sensors in each layer, affecting the throughput of the network and, therefore, its reliability and efficiency.

Option 1: Locating the reference nodes along one side (the coastline) of the lattice of each layer (Figure 2(a)). In this case, the WG needs to traverse only one side. Such a network architecture does not require the WG to enter the water area and simplifies the task of its positioning. However, this architecture can be very inefficient in terms of energy consumption, as the number of retransmissions from the opposite side can be extremely high.

Option 2: Partitioning the orthogonal lattice in each horizontal layer into a finite number of smaller square sublattices (Figure 2(b)). On each sublattice, the ordinary nodes send packets to the central reference node, which in turn sends information vertically through the reference nodes of the other layers on the WG. In doing so, the WG needs to traverse the entire water area and send alerts to the reference nodes of the upper layer to establish communication and receive packets from them. This network architecture may be optimal in terms of energy consumption and prevention of packet bottlenecks. However, it is extremely unprofitable in terms of solving the problem of WG positioning when it sequentially traverses the reference nodes.

Option 3: Deployment of reference nodes along the perimeter of each horizontal layer of the UWASN (Figure 3(a)). In this case, the WG needs to traverse only the perimeter of the water area. A particular case of this arrangement is the perimeter traversal of the inner square of the smaller water area (Figure 3(b)). It can be assumed that traversing the perimeter can be energetically beneficial for small water areas, the traversing of which does not take much time. Traversing the inner square can be optimal for water areas of any size. The smaller the inner square perimeter, the faster the WG can traverse it. However, it is necessary to study this arrangement in terms of energy consumption.

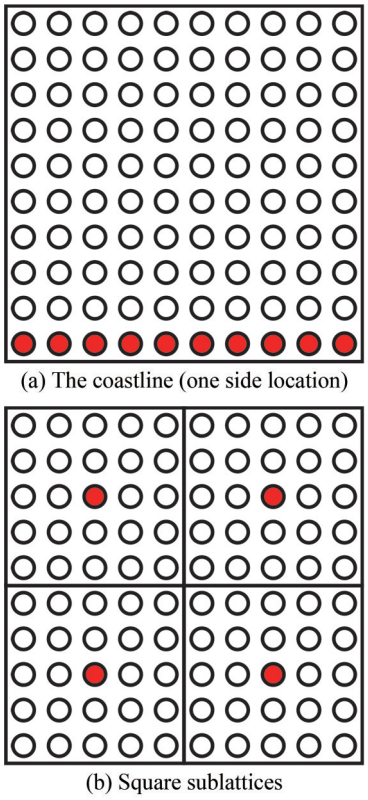

Figure 2 Underwater acoustic sensor network (UWASN) models in an arbitrary layer. The red circles are reference nodes transmitting packets vertically upward to the mobile gateway

To determine the optimal network architecture, a mathematical model is used based on a probabilistic approach (Fedorova et al., 2022) and the criteria for the optimal functioning of the UWASN in terms of connectivity. This considers the restriction on the maximum number of retransmissions N required for successful delivery of the packet.

More specific numerical values for the design parameters used in modeling the UWASN are provided in Section 4. These parameters include the technical characteristics of the transmitting and receiving devices, the network topology, and the physical characteristics of the medium.

4 Design parameters for the UWASN modeling

4.1 Technical characteristics of transmitting and receiving devices

Hydroacoustic communication has severe physical limi-

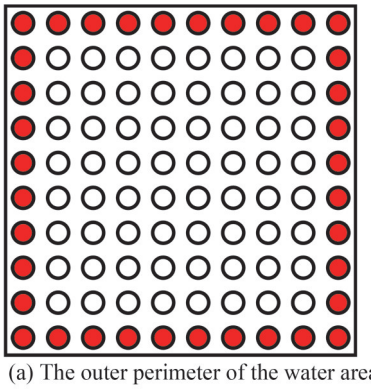

(a) The outer perimeter of the water area

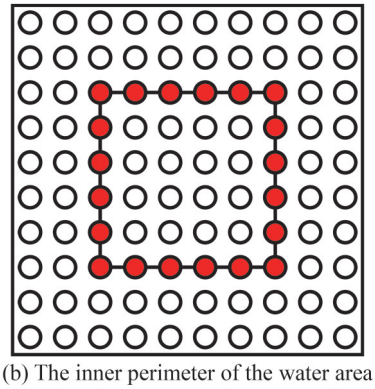

(b) The inner perimeter of the water area (dividing the water area into external and internal parts relative to the reference perimeter)

Figure 3 Underwater acoustic sensor network (UWASN) models in an arbitrary layer. Red circles are reference nodes transmitting packets vertically upward to the mobile gateway

tations on the speed of information transmission due to the narrow bandwidth of the transmitted signals. These limitations are stricter the greater the distance between the sensors. The achievable data rate is limited by Shannon's theorem to the selected bandwidth and the value of the SNR at the receiving antenna. The bandwidth depends on the carrier frequency and the antenna quality coefficient and is usually between 10% and 50% of the carrier frequency. In this work, the central frequency of the modem is taken to be $f = 60$ kHz, the bandwidth is $B = 30$ kHz, the bit rate is $f_{\text{bit}} = 12.8$ kbit/s, and the communication range exceeds 1 000 m.

Hydroacoustic modems with a significantly greater communication range have a lower rate of information transfer, and vice versa; high-speed modems have communication ranges that are much less than that adopted in this work. The modem parameters accepted in this work are selected for the network parameters, are technically realizable at present, and are already implemented in commercial modems (Climent et al., 2014; Zia et al., 2021).

It is assumed that all transmitted packets s have the same length $N_{\text{bit}} = 256$ bits, and in addition to the measured environmental characteristics, the package contains the necessary service information. Then, the total time for packet transmission and confirmation of delivery t_s is determined by the following ratio:

$$t_s = \frac{N_{\text{bit}}}{f_{\text{bit}}} = 0.02 \tag{1}$$

Thus, increasing the bit rate reduces the sending time of the packet and lowers the power inputs at the same transmitted power.

The maximum acoustic power intensity transmitted by the modem antenna is limited to a value of 10 W/cm^2 in water (Margulis and Margulis, 2005). When this power is exceeded, cavitation begins, and the transmitting efficiency drops sharply. Therefore, to increase the acoustic power of the transmitted signal, it is necessary to increase the antenna area. In practice, for a high-speed modem operating at frequencies from 60 kHz to 90 kHz, the geometrical dimensions of the antenna should not be more than 2–2.5 cm^2, and modem power should not exceed the value of 20–25 W. This is because transmission with large antenna dimensions becomes directional, causing the transmission power in certain directions appears several times lower than average, which limits the communication range in that direction (Singh, 2020). In this work, the following energy characteristics of the modem are defined for qualitative and quantitative analysis of the efficiency and reliability of the UWASN (Miguel, 2003):

1) $P_s = 25$ W is the maximum transmitted power of the transmitting modem.

2) $E_s = P_s t_s = 0.5$ J is the energy required to send one packet.

3) $P_w = 0.3$ W is the power spent on waiting for and receiving the packet, an empirical figure for the processor system waiting to receive the packet.

4) $P_{\text{inf}} \approx P_w$ is the power spent on receiving info packets. This is the average power of a running processor system with low energy consumption.

5) $E_0 = 864$ kJ is the capacity of the 12 V battery (Ulvestad, 2018).

4.2 Topology of the network

The network topology is a cubic orthogonal lattice of dimension $n \times n \times m$, with sensors located at its nodes. In this work, we consider two sizes of UWASN: small ($n = 10$) and large ($n = 50$). The third dimension, m, defines the number of layers at a depth of $H = 850$ m where the sensors are located. The simplest configuration consists of $m = 3$ layers, where layer d_0 is near the free surface, layer d_1 is in the water column, and layer d_2 is near the bottom. In the proposed model of the UWASN, the distance between the sensors in the layer is taken as fixed and equal to $r =$ 1 000 m, and the distance between the layers is $h = 400$ m. The upper and lower layers are at $l_{\text{bott}} = 20$ m from the bottom and at $l_{\text{surf}} = 30$ m from the surface, respectively (Figure 1).

4.3 Physical characteristics of the medium

Partitioning into layers allows us to study the dependences of the functional characteristics of the UWASN not only on depth, but also on such physical parameters as the characteristics of waves on the water surface or turbidity and inhomogeneity of suspensions near the bottom. The near-surface layer is very different from the rest of the marine environment (Fox-Kemper et al., 2022). It is characterized by an abnormally high concentration of gas bubbles, which leads to increased sound scattering and absorption, as well as increased acoustic nonlinearity. The scattering coefficient in the bottom layer depends on the particle size distribution and concentration of suspensions and varies significantly depending on the type and concentration of suspended solids.

Estimation of the attenuation coefficient $\beta_0(f)$ in clear water at zero depth at a given sound frequency $f = 60$ kHz is obtained by the Equation (Thorp, 1965):

$$\beta_0(f) = \frac{0.1 f^2}{1 + f^2} + \frac{40 f^2}{4\,100 + f^2} + 2.75 \times 10^{-4} f^2 + 0.000\,3\,(\text{dB/km}) \quad (2)$$

Considering the hydrostatic pressure at depth h (Andreeva, 1975), determined by:

$$\alpha(h) = \left(1 - 6.54 \times 10^{-5} h\right)$$

and empirical estimates of the coefficient k of influence of the bubble layer and muddiness in the upper layer d_0 and suspension near the bottom layer d_2 (Urick, 2013), the following numerical values for the signal attenuation coefficient $\beta = k\alpha(h)\beta_0(f)$ at depth h are obtained:

1) $\beta_0 = 29.3$ dB/km in the upper layer d_0.
2) $\beta_1 = 19.2$ dB/km in the middle layer d_1.
3) $\beta_2 = 26.0$ dB/km in the bottom layer d_2.

The obtained results agree with the empirical data given by Andreeva (1975). Analytical calculations, based on the latest research, can refine the values of β. For instance, considering bubble dynamics (Zhang et al., 2023) can provide a more accurate estimation of the surface layer turbidity. This will be investigated in future studies.

Ambient noise is characterized by the decibel intensity measured with a nondirectional receiver with reference to the intensity of a plane wave in which the root mean square (RMS) pressure is 1 μPa. The noise level in dB using various empirical formulas was estimated by Stojanovic (2007).

The simplest formula gives the approximate linear dependence of noise level in dB on frequency as $10\log_{10} N(f) \approx N_1 - \sigma \log_{10} f$. At parameter values $N_1 = 50$ dB relative to 1 μPa and an empirical coefficient $\sigma = 18$, the noise level at $f = 60$ kHz is 63 dB. The maximum possible value of the noise level in water determined by Stojanovic (2007) is 110 dB. This model assumes that the noise level is constant in each water area for a given season and weather condition.

Following Stojanovic (2007), in this work, we consider not the absolute values of the noise level but the SNR_0, calculated in clear water at $\beta = 0$. Estimates made for the selected modem power $P_s = 25$ W and carrier frequency $f = 60$ kHz, at a distance of $r = 1\,000$ m result in a value of $\text{SNR}_0 = 16.5$ dB.

Section 5 introduces the main new concept—the generalized UWASN connectivity metrics.

5 Generalized UWASN connectivity metrics

Physical layer protocols typically use signal generation and processing algorithms which cannot be changed by the user. Typically, physical layer algorithms make a compromise between data rate and reliability. For example, incoherent signal generation and processing methods provide a high probability of packet delivery and a low probability of bit error but a low data rate (approximately hundreds of bits per second). On the contrary, coherent methods of signal generation and processing are characterized by a high probability of bit error but high data transmission speed (tens of kilobits per second). Incoherent methods provide digital communication in conditions of high variability of the received signal characteristics (Doppler distortion-frequency shift and Doppler spectrum broadening). Coherent methods allow digital communication in conditions of multipath signal scattering, leading to fading and intersymbol interference, but do not allow for high variability of signal reception conditions (they only work well in slowly changing conditions; Kebkal et al., 2019).

The probability of packet reception errors in coherent signal detection can be estimated using the Gaussian error integral:

$$q_{\text{bit}}(x) = \frac{1}{\sqrt{2\pi}} \int_x^{\infty} \exp\left(-\frac{u^2}{2}\right) \mathrm{d}u, \quad x = \frac{a_1 - a_2}{2\sigma_0} \quad (3)$$

In this case, antipode signals with equal energies are transmitted, and the receiver outputs the following components: $a_1 = \sqrt{E_{\text{bit}}}$ for the transmitted signal $s_1(t)$ и $a_2 = -\sqrt{E_{\text{bit}}}$ for the transmitted signal $s_2(t)$, where $E_{\text{bit}} = P_s t_{\text{bit}}$ is the bit energy, $t_{\text{bit}} = 1/f_{\text{bit}}$ is the time expressed in bit rate. For additive white Gaussian noise, the variance σ_0^2 outside the correlator can be replaced by $P_{n_0}/2$, where $P_{n_0} = P_n/B$ is the noise power spectral density. Then, given that the powers relate to each other as squares of the pressures for the variable x included in Equation (2), we have the following.

$$x = \sqrt{\frac{2E_{\text{bit}}}{P_{n_0}}} = \sqrt{\frac{2B}{f_{\text{bit}}}\frac{P_s}{P_n}} = \sqrt{\frac{2B}{f_{\text{bit}}}}\frac{p_s}{n} \tag{4}$$

Here, n is the rms interference pressure at a given frequency. Assuming that the medium is absorbing and the transmitting antenna is nondirectional, the ratio of acoustic pressure at the antenna of the receiving modem to the interference pressure can be expressed as follows:

$$\frac{p_s}{n} = \frac{p_{s_0} r_0}{nr} 10^{-0.05 \cdot \beta \cdot r} \tag{5}$$

where p_{s_0} is the transmitted pressure at a point, with reference to the plane of the transmitting antenna at $r_0 = 1$ m, r is the distance between the transmitting and receiving modems. The pressure of the acoustic signal at the receiving antenna decreases with an increase of distance r and the signal attenuation coefficient β. Given the decibel $\text{SNR}(r) = 20\log_{10}\left(p_{s_0} r_0 / nr\right)$ for the variable x we finally have the following expression:

$$x = \sqrt{\frac{2B}{f_{\text{bit}}}} 10^{0.05(\text{SNR}(r) - \beta \cdot r)} \tag{6}$$

Then, the probability of correct packet reception $p(x)$ when sent once to a neighboring sensor can be calculated as

$$p(x) = 1 - q_{\text{bit}}(x) \tag{7}$$

This probability is only determined by the variable x, which in turn depends on static parameters—technical characteristics of the modem, network topology, and physical parameters of the medium in the water area. It does not depend on dynamic features of the functioning of the whole network, that is, on the selected protocols or dynamic rearrangement of routes. This variable x can be called a generalized network connectivity metric.

Analysis of this metric allows us to choose the network topology and optimal distance between sensors at the first stage of network architecture creation, knowing, for example, the technical characteristics of the modem and physical conditions in the water area.

As a specific example, in this work, we chose a modem operating in the B = 30 kHz frequency band, with a communication bit rate of f_{bit} = 12.8 kbit/s. SNR in the given frequency band was recalculated to the SNR at a distance of 1 km without considering the absorption and scattering coefficients, as equal to SNR_0 = 16.5 dB. Substituting all selected values into the connectivity metric in Eq. (5), we see that one parameter, the distance r between sensors in horizontal layers, remains undefined. Varying it in the range from $500 \leqslant r \leqslant 1\,500$ meters and substituting metric (5) in Equation (6) for package delivery probability, we study the dependence $p(x) = p(r)$. Figure 4 shows the dependence of the single delivery probability $p(r)$ on the distance between sensors r in horizontal layers d_0, d_1, and d_2 at the three corresponding signal attenuation coefficients β_0, β_1, and β_2 defined in Section 4.3.

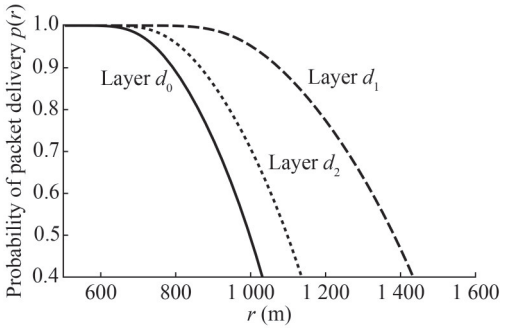

Figure 4 Probabilities of packet delivery as a function of the distance between sensors r for three attenuation coefficients β_0, β_1, and β_2 (in layers d_0, d_1, and d_2, respectively)

Substituting $\beta = 0$ into Equation (5), we see that the choice of the distance between sensors $r = 1\,000$ m provides packet delivery in clear water with 100% probability. Using the previously obtained values of β_0, β_1, and β_2 in each water layer and Equations (5) and (6), we calculate their respective probabilities of packet delivery p_0, p_1, and p_2 in layers with different turbidities. For the model considered in this work, their values are constant, i.e., $p_0 = 0.5$, $p_1 = 0.95$, and $p_2 = 0.7$. The same result can be seen from the graphs (Figure 4).

The obtained values of packet delivery probability for the three considered layers differ with depth. Assume that fewer than 5% of packets are allowed to be lost to ensure successful packet delivery to the gateway. Under this condition, it becomes clear that it is necessary to increase the network capacity for layers d_0 and d_2.

Equations (5) and (6) show how the generalized network connectivity metric x can be changed in two ways to improve network throughput, as follows:

1) Change the modem specifications.

2) Change the network topology by placing the sensors closer to one another.

However, even after selecting the stationary parameters—the technical characteristics of the modem, network topology, and probability of packet delivery to a neighbor under the given water area physical conditions—there is still the possibility of dynamic network optimization by changing the protocol parameters or rearranging routes by partitioning nodes into new clusters.

We now introduce some additional requirements to the routing protocol. Assume that multiple packet retransmissions between sensors are possible. However, if after a fixed number of retransmissions to a neighbor, a particular packet is not delivered, it is considered lost, and the sensor proceeds to forward the next packet in the queue. Let N be the maximum allowed number of retransmissions of one packet

by each sensor. A reasonable choice of the number of retransmissions will increase the probability of packet delivery and, conversely, will reduce the time costs of the network. Then, expression (6) for the probability of correct packet reception can be rewritten as follows:

$$P(x, N) = 1 - q_{\text{bit}}{}^{N}(x) \tag{8}$$

The UWASN architecture assumes a certain number of clusters $M = \{1, 2, \cdots, m\}$. In each cluster, ordinary sensors transmit packets only to their reference node. Consider an arbitrary ith cluster. An ordinary sensor is at the k_ith level of distance from the ith reference node, if k_i hops through other sensors of the cluster are required to deliver a packet from this sensor to the ith reference node. For convenience, we assume that the reference nodes themselves have level $k = 0$. Then, the probability of packet delivery from the k_ith distance level to the reference node, when the probability of cluster connectivity is $P_{k_i}(x, N)$, can be defined by the following expression:

$$P_{k_i}(x, N) = \left[1 - q_{\text{bit}}^{N}(x)\right]^{k_i} \tag{9}$$

Equation (8) shows that the greater the value of distance level k_i, the lower the probability of packet delivery to the reference node and the lower the connectivity of the cluster. Each ith cluster has a sensor that is farthest away. It will take $k_i^{\max}$ hops to the reference node to forward its packet. In other words, we can say that $k_i^{\max}$ is the longest path in the ith cluster or the number of distance levels in that cluster. Let us compare clusters with one another on this feature. Let

$$k_{\max} = \max\left\{k_1^{\max}, k_2^{\max}, \cdots, k_m^{\max}\right\}$$

be the longest path in the whole network. The length of this path can be dynamically changed by changing the location of the reference nodes. Then $P_{k_{\max}}(x, N)$, or the probability of successfully sending a packet to the gateway from the farthest sensor in the whole network, can be considered as a probabilistic criterion of network connectivity. The greater its value, the more reliable and efficient the network will be.

In Section 6, the generalized UWASN connectivity metrics are used to develop a probabilistic mathematical model for network operation.

6 Mathematical model

The aim of this section is to develop a stochastic model of the 3D network functioning to determine and optimize its main characteristics using probabilistic criteria based on the connectivity metric obtained in Section 5. From the standpoint of the stochastic connectivity criterion, the effectiveness of each of the previously proposed arrangements of reference nodes is considered. These arrangements include dividing the network into sublattices with reference nodes located at their centers and placing reference nodes along the perimeter of the water area, along the inner perimeter of the water area, or along one of the sides. Two criteria are defined:

1) A probabilistic criterion of network reliability that estimates the percentage of lost packets in the network. The lower the percentage of lost packets, the higher the reliability of the network.

2) A probabilistic criterion of network efficiency that estimates the total and relative energy consumption for sending all packets to the gateway in one cycle. The lower these consumptions, the more effectively the network operates.

The construction of these criteria for a multilayered 3D area is discussed in Sections 6.1 and 6.2.

6.1 Probabilistic criterion of network reliability

Let the total number of transmissions in the network be denoted by L. Given a probability p of successfully delivering a packet from a sensor to its nearest neighbor and the possibility of sending packets an unlimited number of times, the expected number of transmission attempts between neighboring sensors required for successful delivery is $1/p$. The total expected number of transmissions in an $n \times n$ network can be determined by the following expression:

$$L_p(n) = \frac{L}{p} \tag{10}$$

This approach was used by Fedorova et al. (2022). However, this approach is impractical from a time cost perspective; moreover, from an energy perspective, it is too energy intensive. Therefore, in this work, it is assumed that if a packet is not successfully delivered to all neighbors after a fixed number of transmissions N, it is considered lost, and the sensor moves on to transmitting the next packet in the queue.

As demonstrated in what follows, the introduction of a fixed number N of retransmissions refines the probabilistic formulas and introduces the concept of the packet loss ratio (PLR) as a measure of network reliability. The allowed number of retransmissions N is also included in the probabilistic connectivity criterion $P_{k_{\max}}(x, N)$ and is a crucial parameter in configuring the network's function.

If the number of reference nodes is m, then the number of ordinary nodes, and therefore the number of packets requiring transmission $S(n, m) = n^2 - m$.

All parameters in the metric x in Equation (5) are fixed at the first optimization stage. The only adjustable parameter is the attenuation coefficient β because we are interested in the changes in the delivery probability depending on the

layer depth. We denote the packet loss probability for a single transmission in Equation (2) as $q_{\text{bit}}(x) = q_{\text{bit}}(\beta) = q$, and for N retransmissions, $q^N_{\text{bit}}(x) = q^N_{\text{bit}}(\beta) = q^N = q_1$. The packet delivery probability introduced in Equation (6) is defined as $p(x) = p(\beta) = p = 1 - q$, and the probability introduced in Equation (7) is defined as $P(x, N) = P(\beta, N) = p_1 = 1 - q_1$.

Let $p_k = P_k(x, N) = P_k(\beta, N)$ denote the packet delivery probability from the k-th level of distance to the reference node (see Equation (8)), and let $q_k = 1 - P_k(x, N) = 1 - P_k(\beta, N)$ denote the packet loss probability on that path. Therefore, the delivery of each packet from the kth level of distance follows a Bernoulli distribution with probabilities of success p_k and failure q_k. It follows that:

$$\begin{aligned} p_k &= p_1^k = \left[1 - q^N\right]^k, \\ q_k &= 1 - p_k \quad 1 \leqslant k \leqslant n - 1 \end{aligned} \tag{11}$$

We assume that all ordinary nodes in the network are uniformly divided into clusters; that is, each cluster contains one reference node and the same number of ordinary nodes and has the same levels of distance $k_{\max}$. At each level, they are also uniformly divided into clusters—if there are S_k sensors at level k, then S_k^m sensors will send packets to one reference node, and $S_k = mS_k^m$.

Let PLR denote the average packet loss ratio in the network, that is, the average percentage of packets that are not delivered to the reference nodes. Knowing the probability q_k of losing a packet at the kth level, the number of distance levels in the cluster $k_{\max}$, and the number of packets at each level $S_k(n)$, where $1 \leqslant k \leqslant k_{\max}$, we can obtain a general formula for PLR as a percentage. Substituting its expression (10) instead of q_k and using Equation (8) for the connectivity probability, we finally obtain the network reliability formula as follows:

$$\text{PLR}\left(\beta, n, N, k_{\max}\right) = \sum_{k=1}^{k_{\max}} \frac{S_k(n)}{S(n,m)}\left(1 - P_k(\beta, N)\right) \times 100\% \tag{12}$$

The number of levels $k_{\max}$ and packets on them S_k depends on the specific locations of reference nodes in the network and, in general, depends on the scale of the network $S_k = S_k(n)$.

Thus, in our model, the network reliability depends on the network scale (the water area size) n, the signal attenuation coefficient in the water area β, and on two dynamic parameters—the maximum number of packet retransmissions N and the maximum distance level (maximum packet path length) $k_{\max}$, which is determined by the selected locations of the reference nodes. A detailed analysis of the interdependence of these parameters is provided in what follows.

We assume that the network operates reliably if less than a fraction θ of the total number of packets is successfully delivered to the mobile gateway. This means that the losses can be no more than $1 - \theta$, which leads us to the need to solve the equation:

$$\sum_{k=1}^{k_{\max}} S_k(n) q_k = (1 - \theta)\left(n^2 - m\right)$$

Let $\theta = 0.95$, which means that the losses should exceed $1 - \theta = 0.05$. The corresponding PLR equation is solved graphically for each location of the reference nodes.

In the limit $N \to \infty$, the packet loss probability $q_k \to 0$, and therefore, PLR $\to 0$. This case corresponds to the case presented by Fedorova et al. (2022), where packet losses were not considered.

6.2 Probabilistic criterion of network efficiency

The energy consumption, which depends on the number of packet retransmissions N, can be calculated as follows.

We consider a packet located at the kth level of distance and determine the expected number of retransmissions required to successfully deliver the packet to the reference node. Let η_i be a random variable representing the number of retransmissions of this packet when transmitted from level $k - i + 1$ to level $k - i$, where $1 \leqslant i \leqslant k$. The expected number of retransmissions $\overline{\eta_1}$ from the kth level to the neighboring one (that is, $i = 1$) can be calculated using the formula:

$$\overline{\eta_1} = \sum_{j=1}^{N-1} j q^{j-1} p + N q^{N-1} = \frac{1 - q^N}{p}$$

The distributions η_i for $i > 1$ depend on whether the given packet was successfully delivered to the previous level $k - i + 1$. If it was not (with probability q_{i-1}), then there will be no retransmissions ($\eta_i = 0$); otherwise, the probability must be multiplied by the probability of successful delivery to the previous level p_{i-1}. The average number of retransmissions will be:

$$\overline{\eta_i} = p_{i-1} \frac{1 - q^N}{p}$$

Let $l(\beta, k, N)$ be the average number of hops required to deliver one packet from the kth level of distance to the reference node at the maximum number of retransmissions N. It can be found as follows:

$$l(\beta, k, N) = \sum_{i=1}^{k} \overline{\eta_i} = \frac{1 - p_1^k}{1 - p_1} \frac{p_1}{p}$$

In the limit for an unlimited number of retransmissions $N \to \infty$ the formula simplifies to:

$$l(\beta, k, \infty) = \frac{k}{p}$$

Knowing the number of levels $k_{\max}$ and the number of packets on each level S_k, where $1 \leqslant k \leqslant k_{\max}$, we can obtain a general formula for the total number of transmissions in the network:

$$L(\beta, n, N, k_{\max}) = \sum_{k=1}^{k_{\max}} S_k(n)\, l(\beta, k, N)$$

Substituting the expression for $l_p(k, N)$ into this formula and using Equations (7) and (8), we can finally obtain the total number of transmissions:

$$L(\beta, n, N, k_{\max}) = \sum_{k=1}^{k_{\max}} S_k(n) \frac{1 - P_k(\beta, N)}{1 - P(\beta, N)} \frac{P(\beta, N)}{p(\beta)} \quad (13)$$

If the power consumption for waiting for and receiving packets is negligible ($P_w \approx 0$), we can focus only on the energy consumption required for packet transmission. This assumption allows us to neglect the energy consumption for listening to the channel and waiting for packets. By doing so, we can compare different arrangements more efficiently in terms of the number of retransmissions. The total energy consumption of such an ideal network is only related to the energy consumed for packet transmission:

$$E(\beta, n, N, k_{\max}) = L(\beta, n, N, k_{\max}) P_s t_s \quad (14)$$

The higher the network load, the closer the actual network performance is to the ideal network functioning, as much of the time is indeed spent on packet transmission rather than waiting.

If we divide the average energy consumption for a finite number of retransmissions N by the maximum possible energy consumption at an unlimited number of retransmissions, we can obtain the equation for the relative energy consumption:

$$\varepsilon(\beta, n, N, k_{\max}) = \frac{E(\beta, n, N, k_{\max})}{E(\beta, n, \infty, k_{\max})} \times 100\% \quad (15)$$

So, all probabilistic criteria developed and constructed as part of the connectivity metric are expressed by Equations (11), (13), and (14) and contain the following two sets of parameters:

1) The signal attenuation coefficient in the water area β and the network scale n, which are static nonadjustable system parameters.

2) The maximum number of packet retransmissions N allowed by the selected protocol and the maximum number of distance levels in the cluster $k_{\max}$, which are dynamically adjustable system parameters.

Assuming the static parameters to be predetermined, Section 7 presents a concept for selecting the optimal packet routing in the UWASN depending on the selected dynamic parameters.

7 Reference nodes location

In this section, the constructed reliability (Equation (11)), total energy consumption (Equation (13)), and relative energy consumption (Equation (14)) criteria will be applied to various reference nodes placement in the network, considering various maximum allowed retransmissions N.

7.1 Coastline (one side location)

The first option to consider is the case where the reference nodes are placed along one side of the grid, as shown in Figure 2(a). For simplicity, we assume that on the selected side of the grid, all sensors in each layer are reference nodes, that is,

$$m = n, \quad S = n^2 - n, \quad k_{\max} = n - 1$$

In this case, we have $S_k = n$ packets at levels $k = 1, 2, \cdots, n - 1$. Thus, using Equation (11), we obtain the average percentage of lost packets as

$$\mathrm{PLR}(\beta, n, N) = \frac{\left(1 - q_{\mathrm{bit}}^N(\beta)\right)^n + n q_{\mathrm{bit}}^N(\beta) - 1}{(n - 1) q_{\mathrm{bit}}^N(\beta)} \times 100\%$$

Fedorova et al. (2022) showed that placing reference nodes along one of the sides could only be effective in the case of small-scale networks. Therefore, in this work, we investigate the case of $n = 10$.

Figure 5 shows PLR as a function of the maximum number of retransmissions N at different layers of the water area. Here and in the remainder of Section 7, we assume that in the upper near-surface layer of sensors d_0, the packet delivery probability is low and equal to $p = 0.5$; in the middle layer of sensors located in the water column d_1, the packet delivery probability is high and equal to $p = 0.95$; and in the lower bottom layer of sensors d_2, the packet delivery probability is equal to $p = 0.7$.

Figure 5 shows that in the middle layer of sensors d_1, with $p = 0.95$, almost all packets will be delivered to the reference nodes with two retransmissions. However, in the lower layer of sensors d_2, with $p = 0.7$, approximately 40% of packets will be lost in the network with two retransmissions. In the upper layer of sensors d_0, with $p = 0.5$, most packets will be lost with two retransmissions. The situation significantly improves with four retransmissions, and with 10 retransmissions, the delivery of all packets can be expected. Thus, we observe a strong dependence of the

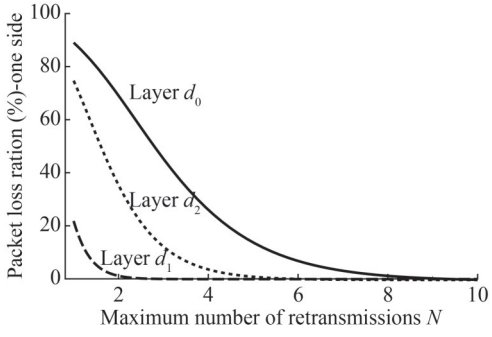

Figure 5 Average PLR as a function of the maximum number of retransmissions N (layers d_0, d_1, and d_2, $n = 10$), one side reference nodes location

required number of retransmissions on the depth of the sensor layer.

However, as the number of retransmissions increases, the energy consumption in the network also increases. To calculate the energy consumption, it is necessary to determine the average number of retransmissions in the network using Equation (12), which in this case gives the expression:

$$L(\beta, n, N) = n\frac{P(\beta, N)}{p(\beta)}\sum_{k=1}^{n-1}\frac{1 - P_k(\beta, N)}{1 - P(\beta, N)} \qquad (16)$$

where multiplying the right-hand side by $P_s T_s$ according to Equation (13), we obtain the average energy consumption $E(\beta, n, N)$. In the limit $N \to \infty$, Equation (10) takes the form:

$$L(\beta, n, \infty) = \frac{(n^3 - n^2)}{2p(\beta)}$$

This result coincides with the one obtained by Fedorova et al. (2022).

Figure 6 shows the average energy consumption as a function of the maximum number of retransmissions N at different layers of the water area.

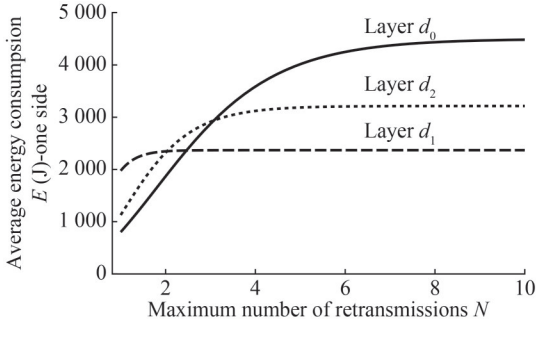

Figure 6 Average energy consumption E as a function of the maximum number of retransmissions N (layers d_0, d_1, and d_2, $n = 10$), one side reference nodes location

For any network configuration, there is a limiting number of retransmissions $N \approx 10$, at which energy consumption stops increasing and tends toward its limiting value, which was obtained by assuming $N \to \infty$.

The relative energy consumption can be obtained by Equation (14) as follows:

$$\varepsilon(\beta, n, N) = \frac{2P(\beta, N)}{n^2 - n}\sum_{k=1}^{n-1}\frac{1 - P_k(\beta, N)}{1 - P(\beta, N)} \times 100\% \qquad (17)$$

Equation (17) is used to compare different reference nodes deployment.

7.2 Regular sublattices

The case of splitting the network into equal sublattices of the same dimensions is also of interest. This case is shown in Figure 2(b). We assume that each sublattice is a square grid of dimension $l \times l$, where l is an odd number. Reference nodes are in the centers of these sublattices. To simplify the calculations, we assume that n^2 is divisible by l^2, that is, $n^2 = m \times l^2$ (where m is the number of reference nodes). The dependence of the number of packets S_k at each level on the side length l of the sublattice, can be described by:

$$S_k = 4m\min(k, l - k),\ 1 \leqslant k \leqslant l - 1,$$
$$k_{\max} = l - 1$$

Using Equation (11), we can find the average percentage of lost packets:

$$\mathrm{PLR}(\beta, l, N) = \frac{4}{l^2 - 1}\sum_{k=1}^{l-1}\min(k, l - k)\left(1 - P_k(\beta, N)\right) \times 100\%$$

PLR does not depend on the network size n, but only on the sublattice size l.

For simplicity, only sublattices of a dimension $l = 5$ are considered. In this case, for a small network, we have $m = 4$, and for a large network, we have $m = 100$ reference nodes. This sublattice has four levels of distance between the regular sensors and the reference nodes: four sensors on the first and fourth levels and eight sensors on the second and third levels. Taking this into account, we obtain the following expression for the average percentage of lost packets:

$$\mathrm{PLR}(\beta, N) = \frac{50}{3}q_{\mathrm{bit}}^N(\beta) \times\left(15 - 14q_{\mathrm{bit}}^N(\beta) + 6q_{\mathrm{bit}}^{2N}(\beta) - q_{\mathrm{bit}}^{3N}(\beta)\right)$$

Figure 7 shows PLR as a function of the maximum number of retransmissions N at different layers of the water area (in this case, there is no dependence on the network size).

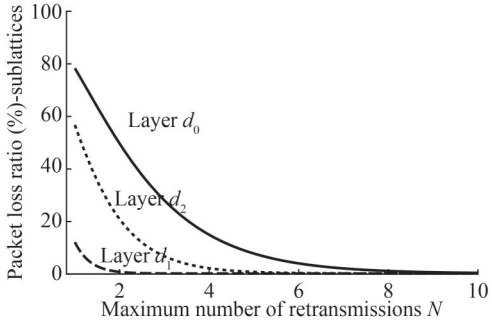

Figure 7 Average PLR as a function of the maximum number of retransmissions N (layers d_0, d_1, and d_2), reference nodes located at the centers of regular sublattices

In the middle layer of sensors d_1, almost all packets will be delivered to the reference nodes with two retransmissions. In the lower layer of sensors d_2, approximately 20% of packets will be lost in the network with two retransmissions (this percentage was significantly higher when the reference nodes were placed on one side). In the upper layer of sensors d_0, half of the packets will be lost with two retransmissions. The situation significantly improves with four retransmissions. With $N \approx 10$, the delivery of all packets can be expected. In terms of packet delivery reliability, dividing the network into sublattices proves to be better than placing the reference nodes on one side.

To estimate the energy consumption, the average number of retransmissions in the network is determined using the general Equation (12):

$$L(\beta, l, m, N) = \frac{4m\left(1 - q_{\text{bit}}^{N}(\beta)\right)}{p(\beta)q_{\text{bit}}^{N}(\beta)} \times \sum_{k=1}^{l-1} \min(k, l-k)\left(1 - P_k(\beta, N)\right)$$

Considering the case of $l = 5$ simplifies the expression to:

$$L(\beta, m, N) = \frac{4m}{p(\beta)}\left(1 - q_{\text{bit}}^{N}(\beta)\right) \times \left(15 - 14q_{\text{bit}}^{N}(\beta) + 6q_{\text{bit}}^{2N}(\beta) - q_{\text{bit}}^{3N}(\beta)\right)$$

Multiplying the right-hand side by $P_s T_s$ using Equation (13), we obtain the average energy consumption $E(\beta, m, N)$. In contrast to the percentage of lost packets, the total energy consumption depends on the network size. In this case, we consider a large network ($n = 50$). As shown in Fedorova et al. (2022), it is more efficient to partition a large network into sublattices than to place the reference nodes along one side.

In the limit $N \to \infty$, the formula takes the form:

$$L(\beta, m, \infty) = 4m \sum_{k=1}^{l-1} \min(k, l-k)\frac{k}{p}$$

Figure 8 shows the average energy consumption as a function of the maximum number of retransmissions N at different layers of the water area for a large network ($n = 50$).

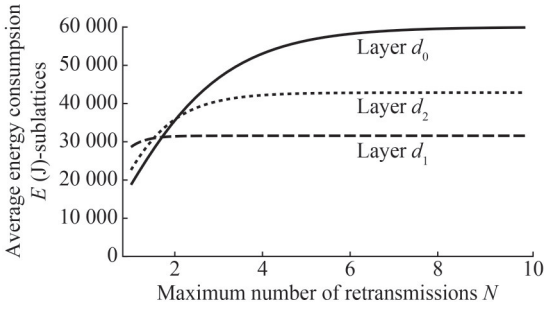

Figure 8 Average energy consumption E as a function of the maximum number of retransmissions N (layers d_0, d_1, and d_2, $n = 50$), reference nodes located at the centers of regular sublattices

There is a limiting number of retransmissions $N \approx 10$, at which energy consumption stops increasing and tends toward its maximum value. It is not possible to compare these results with those of the previous arrangement as they are studied on networks of different scales.

Therefore, we calculate relative energy consumption, which is used in the last section to plot comparative graphs. The relative energy consumption at $l = 5$ can be obtained by Equation (14):

$$\varepsilon(\beta, N) = \frac{1}{15}\left(1 - q_{\text{bit}}^{N}(\beta)\right) \times \left(15 - 14q_{\text{bit}}^{N}(\beta) + 6q_{\text{bit}}^{2N}(\beta) - q_{\text{bit}}^{3N}(\beta)\right)$$

The relative energy consumption, in this case, does not depend on the network size.

7.3 Outer perimeter of water area

The case of locating the reference nodes on the outer perimeter is shown in Figure 3(a). We assume that all nodes located on the outer perimeter of the network are reference nodes. The total number of reference nodes will be $m = 4(n-1)$. The number of levels of distance between the ordinary sensors and the reference nodes depends on the evenness of n. For simplicity, only the case of even n is considered so that the number of levels can be determined by:

$$k_{\max} = \frac{n}{2} - 1, \quad n = 2j$$

The number of packets on each level, in this case, is calculated as follows:

$$S_k = 4(n - 2k - 1), \quad 1 \leqslant k \leqslant k_{\max}$$

Using Equation (11), we can find the average percentage of lost packets:

$$\text{PLR}(\beta, n, N) = \sum_{k=1}^{\frac{n}{2}-1} \frac{4(n-2k-1)}{n^2 - 4(n-1)}\left(1 - P_k(\beta, N)\right) \times 100\%$$

Calculating the sum, we obtain:

$$\mathrm{PLR}(\beta, n, N) = \frac{100}{(n-2)^2 q_1^2} \times \left(n^2 q_1^2 + 4q_1\left((1-q_1)^{n/2} - n - 1 \right) - 8 + 8(1-q_1)^{n/2} \right)$$

where $q_1 = q_{\mathrm{bit}}^N(\beta)$.

Fedorova et al. (2022) showed that placing the reference nodes on the outer perimeter can be effective only for small networks. Therefore, we will only consider the case of $n = 10$.

Figure 9 shows PLR as a function of the maximum number of retransmissions N at different layers of the water area.

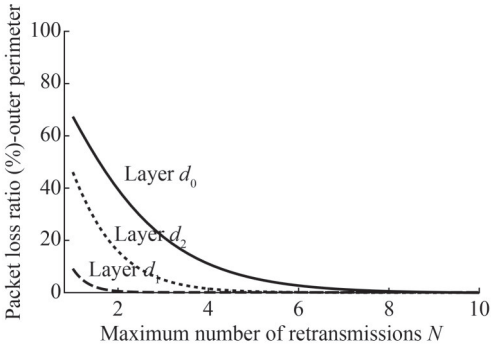

Figure 9 Average PLR as a function of the maximum number of retransmissions N (layers d_0, d_1, and d_2, $n = 10$), outer perimeter reference nodes location

The graphs show that in the middle layer of sensors d_1, almost all packets will be delivered to the reference nodes with two retransmissions. However, in the lower layer of sensors d_2, approximately 20% of packets will be lost with two retransmissions. In the upper layer of sensors d_0, approximately 40% of packets will be lost with two retransmissions. With four retransmissions, the situation improves significantly, and at $N \approx 10$, it is expected that all packets will be delivered. However, with an increase in the number of retransmissions, the energy consumption in the network also increases.

The average number of retransmissions in the network for even n is determined using Equation (12):

$$L(\beta, n, N) = \frac{1 - q_{\mathrm{bit}}^N(\beta)}{p(\beta) q_{\mathrm{bit}}^N(\beta)} \times \times \sum_{k=1}^{\frac{n}{2}-1} 4(n - 2k - 1)\left(1 - P_k(x, N)\right)$$

Calculating the sum, we obtain:

$$L(\beta, n, N) = \frac{1-q_1}{p q_1^3}\left(n^2 q_1^2 + 4q_1\left((1-q_1)^{n/2} - n - 1 \right) - 8 + 8(1-q_1)^{n/2} \right)$$

Multiplying the right-hand side by $P_s T_s$ using Equation (13), we obtain the average energy consumption $E(\beta, n, N)$.

In the limit $N \to \infty$, the formula takes the following form:

$$L(\beta, n, \infty) = \frac{1}{6p}\left(n^3 - 3n^2 + 2n \right)$$

This coincides with the result obtained by Fedorova et al. (2022).

Figure 10 shows the average energy consumption as a function of the maximum number of retransmissions N at different layers of the water area for a small network ($n = 10$).

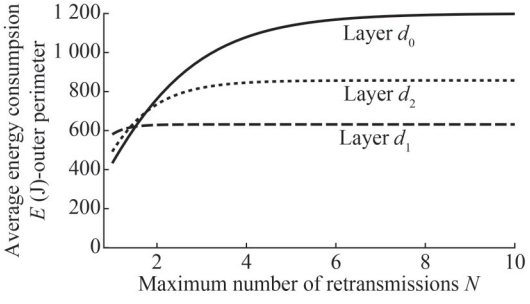

Figure 10 Average energy consumption E as a function of the maximum number of retransmissions N (layers d_0, d_1, and d_2, $n = 10$), outer perimeter reference nodes location

As in the previous cases (Fedorova et al., 2022), for a given network configuration, there is a limiting number of retransmissions $N \approx 10$, at which energy consumption stops increasing and tends toward its maximum value. We cannot compare them with the previous arrangements because they are studied on networks of different scales.

To compare arrangements, we can calculate the relative energy consumption using Equation (14):

$$\varepsilon(\beta, n, N) = \frac{6}{n^3 - 3n^2 + 2n} \frac{1-q_1}{q_1^3} \times \left(n^2 q_1^2 + 4q_1\left((1-q_1)^{\frac{n}{2}} - n - 1 \right) - 8 + 8(1-q_1)^{\frac{n}{2}} \right) \times 100\%$$

where $q_1 = q_{\mathrm{bit}}^N(\beta)$.

7.4 Inner perimeter of water area

The case of locating the reference nodes on an arbitrary inner perimeter is shown in Figure 3(b). Placing the reference nodes on the outer perimeter works well for small networks but ceases to be an optimal arrangement for large networks. This is because the parameter $k_{\max}$ becomes exceptionally large, and ordinary sensors must make many transmissions to the perimeter where the reference nodes are located. For large networks, dividing them into sublattices becomes more optimal. However, such an arrange-

ment of reference nodes has a significant disadvantage related to the necessity of positioning more than one WG at different internal points of the water area over the reference nodes.

Therefore, it is proposed to allocate an inner perimeter of the water area for the reference nodes. In this case, the WG will need to be positioned on the perimeter of the square, which is not as difficult as navigating all the sublattices. But the number of transmissions $k_{\max}$ to the inner perimeter will be much smaller than to the outer perimeter.

To simplify the calculations, the reference nodes are supposed to be located inside the water area on a square perimeter such that the center of the square coincides with the center of the network. Let n be even, $n = 2v$. Then, the number of possible perimeters for placing reference nodes will be equal to v. These perimeters can be numbered, starting from the inner square, and we assume that the reference nodes are located on the μth perimeter, $1 \leqslant \mu \leqslant v$. The number of reference nodes will be $m = 4(2\mu - 1)$, and the number of packets to be delivered to the reference nodes will be

$$S = n^2 - 4(2\mu - 1)$$

The ordinary sensors can be divided into external and internal sensors with respect to the reference nodes. Accordingly, the task of determining the number $k_{\max}$ of levels of distance between ordinary sensors and the reference nodes, as well as the number of packets at each level S_k, also can be divided into two parts (Figure 3(b)). Let $k_{\max}^{\text{in}}$, S_{k}^{in}, $k_{\max}^{\text{out}}$, S_k^{out} denote these characteristics.

The determination of $k_{\max}^{\text{in}}$ and S_k^{in} is made as in the case of the outer perimeter with the even grid size:

$$k_{\max}^{\text{in}} = \mu - 1$$
$$S_k^{\text{in}} = 4(2\mu - 2k - 1), \quad 1 \leqslant k \leqslant k_{\max}^{\text{in}}$$

The values of $k_{\max}^{\text{out}}$ and S_k^{out} are determined by:

$$k_{\max}^{\text{out}} = 2(v - \mu)$$
$$S_k^{\text{out}} = 4 \times \begin{cases} 2\mu + k - 1, & 1 \leqslant k \leqslant \dfrac{k_{\max}^{\text{out}}}{2} \\ 2v - (2\mu + k - 1), & \dfrac{k_{\max}^{\text{out}}}{2} + 1 \leqslant k \leqslant k_{\max}^{\text{out}} \end{cases}$$

Using Equation (11), we can find the average percentage of lost packets:

$$\text{PLR}\left(\beta, n, N, k_{\max}^{\text{in, out}}\right) = \left(\sum_{k=1}^{k_{\max}^{\text{in}}} \frac{S_k^{\text{in}}}{S}\left(1 - P_k(\beta, N)\right) + \sum_{k=1}^{k_{\max}^{\text{out}}} \frac{S_k^{\text{out}}}{S}\left(1 - P_k(\beta, N)\right)\right) \times 100\%$$

The PLR curves for all possible square perimeters μ are shown in Figure 11, considering the small network ($n = 10$) and placement of the sensors in layer d_0. When $\mu = 5$, the perimeter coincides with the perimeter of the water area.

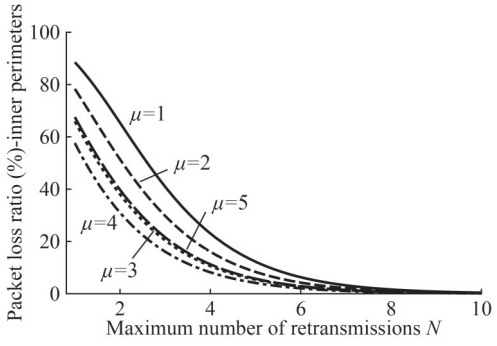

Figure 11 Average PLR as a function of the maximum number of retransmissions N (upper layer d_0, $n = 10$, $p = 0.5$), inner perimeter reference nodes location

From the graph, the highest PLR is observed for the smallest perimeter $\mu = 1$ and the next one for $\mu = 2$. The best result is observed for the perimeter $\mu = 4$. This result is also observed in the other layers at different depths (data not shown).

In the case of a large network ($n = 50$) with a total number of inner perimeters $\mu = 25$, it is not expedient to plot such a large quantity of graphs. Therefore, the optimal values of μ were numerically determined for different combinations of the number of transmissions N and packet delivery probabilities p. It was found that this range is $19 \leqslant \mu \leqslant 21$, depending on the chosen value of N.

Because the scale of the network is even ($n = 2v$), the number of retransmissions consists of two terms:

$$L\left(\beta, n, N, k_{\max}^{\text{in, out}}\right) = \sum_{k=1}^{k_{\max}^{\text{in}}} S_k^{\text{in}}\, l(k, N) + \sum_{k=1}^{k_{\max}^{\text{out}}} S_k^{\text{out}}\, l(k, N)$$

Multiplying the right-hand side by $P_s T_s$ using Equation (13), we obtain the average energy consumption.

The average energy consumption as a function of the maximum number of retransmissions N for different values of μ in a small network ($n = 10$) are shown in Figure 12, for the upper layer d_0.

The highest energy consumption is observed for the smallest perimeter $\mu = 1$ and the next highest for $\mu = 2$. Again, the best result is observed for the second-to-last perimeter, $\mu = 4$. This result is also observed in the other layers at different depths (data not shown).

For a large network ($n = 50$) and a total number of inner perimeters $\mu = 25$, the optimal μ values were found numerically for different combinations of the number of retransmissions N and packet delivery probabilities p. This range is again $19 \leqslant \mu \leqslant 21$ depending on the chosen value of N.

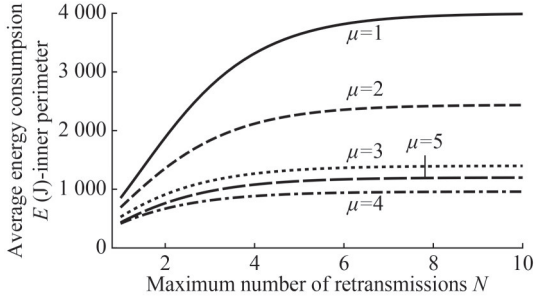

Figure 12 Average energy consumption E as a function of the maximum number of retransmissions N (layer d_0, $n = 10$, $p = 0.5$), inner perimeter reference nodes location

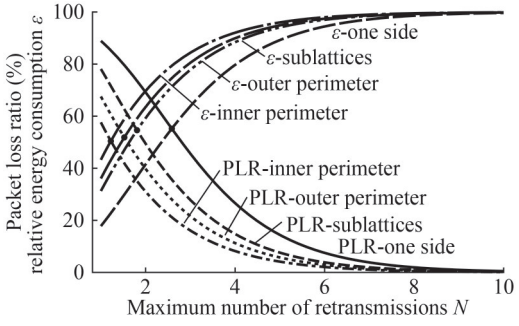

Figure 13 Average PLR and relative energy consumption ε as functions of the maximum number of retransmissions N (layer d_0, $n = 10$, $p = 0.5$) for all reference nodes arrangements

Further, for comparison of the inner perimeter arrangement with the other arrangements, we take $\mu = 4$ for a small network ($n = 10$) and $\mu = 19$ for a large network ($n = 50$).

The relative energy consumption can be obtained by Equation (14):

$$\varepsilon\left(\beta, n, N, k_{\max}^{\text{in, out}}\right) = \frac{L\left(\beta, n, N, k_{\max}^{\text{in, out}}\right)}{L\left(\beta, n, \infty\right)} \times 100\%$$

In Section 8, a comparison of node arrangements will be conducted for different scales in terms of the criteria of energy efficiency and reliability.

8 Comparisons of different reference node arrangements

In Section 7, we investigated each reference node arrangement in terms of efficiency and reliability criteria, depending on the network size and layer depth. In this section, the performances of different arrangements of reference nodes are compared using these criteria at different scales.

8.1 Small networks

In this section, a small network ($n = 10$) in the upper layer of sensors d_0 ($p = 0.5$) is considered.

Figure 13 shows comparative graphs of PLR and the relative energy consumption ε as a function of the maximum number of retransmissions N.

In Figure 13, the equilibrium points are found where the curves of the PLR and relative energy consumption intersect. This point corresponds to a value of 50% to 55% for all arrangements, that is, slightly more than half of the delivered packets at half of the maximum possible network load. As the number of retransmissions N increases, the network's reliability increases because the proportion of successfully delivered packets increases, but the efficiency of the network decreases because energy consumption increases. The curves in Figure 13 are qualitative and do not allow for a rigorous quantitative analysis, but they provide a visual comparison of the reference nodes arrangements. The number of transmissions required to reach the equilibrium point varies. The least efficient option in terms of the location of the equilibrium point is when the reference nodes are located along one side. Consecutive improvements in efficiency for small networks are seen when dividing the network into sublattices, followed by locating them along the perimeter. The most efficient arrangement is when the reference nodes are located on the inner perimeter. In Figure 13, the equilibrium point for this arrangement lies to the left of all others.

Thus, if the physical conditions in the water area are known, the protocol can be adjusted separately for each network to ensure the required level of reliability and efficiency.

In the other layers, the locations of the curves on the comparative graphs remain the same. This suggests that locating the reference nodes on the inner perimeter is optimal for small networks in any layer when using modems with identical technical characteristics and the same protocol settings for the number of retransmissions N. This arrangement provides higher reliability and efficiency of network operation than the others.

A comparative analysis of the total energy consumption for various arrangements for a small network in the upper layer of sensors d_0 is shown in Figure 14.

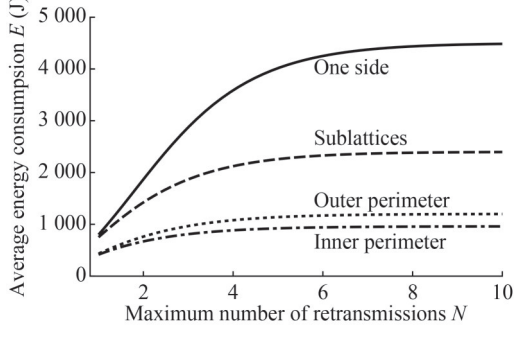

Figure 14 Total energy consumption E as a function of the maximum number of retransmissions N (layer d_0, $n = 10$, $p = 0.5$) for all reference nodes arrangements

The most energy consumption in small networks occurs for the arrangement of reference nodes along one side, followed by dividing the network into sublattices and then by locating the reference nodes on the outer perimeter. The most energy-efficient arrangement is where the reference nodes are on the inner perimeter. This result is also observed in the other layers, although the absolute values of energy consumption vary—the lower the packet delivery probability, the higher the energy consumption.

The network is assumed to be reliable if it ensures successful delivery of 95% of packets.

A quantitative comparison of the reference nodes arrangements is presented in Table 1. To obtain meaningful results when filling in the table, it is necessary to round up the maximum number of retransmissions using the ceiling function, $\lceil N \rceil$. In addition, we assume that the number of transmissions is always $\lceil N \rceil \geqslant 2$, even if the graph gives us a value of $N \approx 1$.

The best characteristics are highlighted in bold in Table 1. For an arbitrarily unlimited water area, the deployment of reference nodes along the inner perimeter has the best characteristics for small networks.

8.2 Large networks

In this section, a large network ($n = 50$) in the upper layer of sensors d_0 ($p = 0.5$) is considered.

Figure 15 shows PLR and the relative energy consumption ε as functions of the maximum number of retransmissions N.

In a large network, the situation changes significantly compared to the results obtained for a small network. The equilibrium points for all arrangements correspond to a value of approximately 55%; that is, slightly more than half of the packets are delivered at half of the maximum possible network load. However, the number of required retransmissions changes but the least efficient arrangement in terms of the equilibrium point location remains that of placing the reference nodes along one side. The next least efficient arrangement for large networks is the outer perimeter, followed by placement on the inner perimeter. The most efficient option is dividing the network into sublattices.

In the other layers, the positions of the curves on the comparative graphs remain the same. From this, it can be concluded that dividing the network into sublattices is the optimal arrangement for large-scale networks when using modems with the same technical specifications and the same protocol settings for the number of retransmissions N. This arrangement provides higher reliability and efficiency of network operation than the others.

A comparative analysis of the total energy consumption for various arrangements for a large network in the upper layer of sensors d_0 is shown in Figure 16.

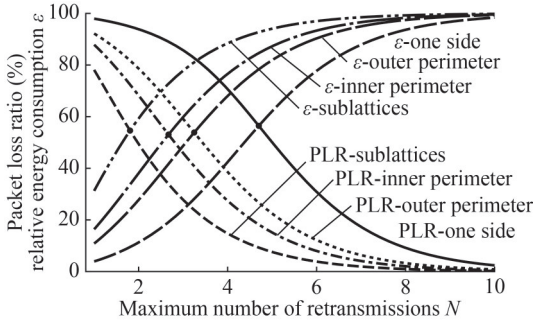

Figure 15 Average PLR and relative energy consumption ε as functions of the maximum number of retransmissions N (layer d_0, $n = 50$, $p = 0.5$) for all reference nodes arrangements

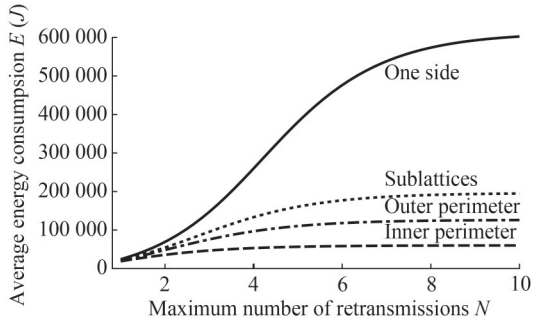

Figure 16 Total energy consumption E as a function of the maximum number of retransmissions N (layer d_0, $n = 50$, $p = 0.5$) for all reference nodes arrangements

The order of the curves in Figure 16 is the same as in Figure 14. Thus, the analysis of the graphs of the total energy consumption confirms that for large networks, dividing the three-dimensional lattice into a finite number of sublattices is the most advantageous arrangement in terms of efficiency and reliability. However, as mentioned previously, this architecture requires several wave gliders acting as mobile gateways in the hybrid UWASN.

We assume that the network is reliable if it ensures the successful delivery of 95% of packets. A quantitative comparison of the considered arrangements is presented in Table 2.

Table 1 Required number of retransmissions N and energy consumption E for PLR = 0.95 (layers d_0, d_1, d_2, $n = 1$)

Reference node arrangement	Upper layer of sensors d_0			Bottom layer of sensors d_2			Middle layer of sensors d_1		
	N	$\lceil N \rceil$	E (kJ)	N	$\lceil N \rceil$	E (kJ)	N	$\lceil N \rceil$	E (kJ)
Along one side	6.6	7	4.4	3.8	4	3.2	1.5	2	2.4
In the centers of the sublattice	5.6	6	2.4	3.2	4	1.7	1.3	2	1.3
On the outer perimeter	5.2	6	1.2	3.0	3	0.9	1.2	2	0.7
On the inner perimeter	4.7	5	1.0	2.7	3	0.7	1.1	2	0.6

Table 2 Required number of retransmissions N and energy consumption E for PLR = 0.95 (layers d_0, d_1, d_2, $n = 50$)

Reference nodes arrangement	Upper layer of sensors d_0			Bottom layer of sensors d_2			Middle layer of sensors d_1		
	N	$\lceil N \rceil$	E (kJ)	N	$\lceil N \rceil$	E (kJ)	N	$\lceil N \rceil$	E (kJ)
Along one side	8.9	9	593	5.1	6	433	2.1	3	322
in the centers of the sublattice	5.6	6	59	3.2	4	43	1.3	2	32
On the outer perimeter	7.4	8	192	4.2	5	138	1.7	2	102
On the inner perimeter	6.7	7	123	3.9	4	88	1.6	2	66

The best features are highlighted in bold in Table 2. Dividing the 3D lattice into a finite number of sublattices is the best arrangement of the reference nodes for large networks.

Comparing the results in Tables 1 and 2, the following conclusions can be drawn. Dividing the 3D lattice into sublattices provides decent analytical results for large networks, but it may be impractical for hybrid networks due to difficulties with positioning the wave gliders. The best WG movement option for networks of any scale turned out to be following an internal square contour with a side of 0.8 of the network's characteristic size. It provides satisfactory results in terms of network reliability and efficiency and does not cause difficulties with WG movement. Network reliability is determined by the PLR. The requirement set in the study is that PLR should not exceed 5%. Based on this requirement, the optimal number of retransmissions N was selected depending on the network scale $n \times n$ and the depth of sensor placement d_i in the water area. The developed criteria of reliability and efficiency made it possible to determine that for a small network ($n = 10$), two retransmissions ($N = 2$) with energy consumption of $E = 0.6$ kJ will be required to ensure the specified PLR in the middle layer, three retransmissions ($N = 3$) with $E = 0.7$ kJ in the lower layer, and five retransmissions ($N = 5$) with $E = 1.0$ kJ in the upper layer. Similar calculations for a large network $n = 50$ resulted in two retransmissions ($N = 2$) with energy consumption of $E = 66$ kJ in the middle layer, four retransmissions ($N = 4$) with $E = 88$ kJ in the lower layer, and seven retransmissions ($N = 7$) with $E = 123$ kJ in the upper layer. Reducing energy consumption in this case will lead to an increase in PLR and, accordingly, a decrease in network reliability.

9 Conclusions

A new stochastic characteristic of the functioning quality of UWASNs called connectivity has been proposed. Unlike well-known metrics, it covers both static technical and topological parameters of the network and the physical environmental conditions, as well as dynamic characteristics of the network, which allows us to configure and modify the network after it is launched. This characteristic lets us describe a wide range of problems that arise when studying the functioning of UWASNs at the stages of collecting, transmitting, and processing information by sensor devices.

Stochastic characteristics of network connectivity are introduced, which, unlike known ones, describe the whole network rather than the properties of its individual elements.

Criteria for the reliability and efficiency of network functioning have been developed based on the UWASN connectivity, considering physical parameters such as the attenuation coefficient β in the water area, the network scale n, and dynamically changing system parameters such as the number of packet retransmissions N in the selected protocol and the maximum number of levels of distance in the cluster k_{max}.

The developed criteria make it possible to improve the assessment of the quality of the wireless sensor network function.

In this work, using the developed criteria, a comparative analysis of network reliability and power consumption is conducted depending on the maximum number of retransmissions of packets N, determined for different layers of the water area. Analyses were performed for the cases of small ($n = 10$) and large ($n = 50$) networks for four possible arrangements of reference nodes corresponding to water areas traversed by a wave glider. These models unclude glider movement along one side, traversing the perimeter of the water area, traversing the inner perimeter of the water area, and traversing the reference nodes in the sublattices of the 3D lattice.

When considering the selected network architecture, some simplifying assumptions were made. It is assumed that the reference nodes in the layers are located strictly below one another to reduce losses when transmitting packets to the glider. In addition, servicing the water area with only one glider is considered, which imposes restrictions on the scale of the network. More complex cases will be investigated in future works.

The equilibrium points where the curves for PLR and relative energy consumption cross were found. For all arrangements of the reference nodes, these points correspond to values of 50%–55%, but the number of required retransmissions N varies for different arrangements. Thus, the proposed graphs allow us to choose the optimal combination of network dynamic parameters.

Therefore, if the physical conditions in the water area are known, it is possible to adjust the protocol for each arrange-

ment of reference nodes in accordance with the graphs in this work to ensure the required level of reliability and efficiency. Optimal trajectories for the wave glider's movement have been determined in terms of ensuring the efficiency and reliability of hybrid UWASNs of various scales. An evaluation of different reference node arrangements was conducted to ensure packet transmission to a mobile gateway. Analysis of the calculation results showed that the best arrangement of reference nodes, related to the dynamic capabilities of the wave glider, is on an internal square contour with a side of 0.8 of the network size. Such an arrangement is optimal for networks of any scale.

Further work is planned within the framework of the developed criteria to select the technical characteristics of transmitting devices, such as data transmission rate and carrier frequency, as well as global characteristics of the network, such as temporal protocols, the distance between sensors, and the total number of sensors in the water area.

The proposed criteria allow for not only qualitative but also quantitative evaluations of network efficiency and reliability.

Acknowledgement The research is partially funded by the Ministry of Science and Higher Education of the Russian Federation as a part of World-class Research Center Program: Advanced Digital Technologies (contract No. 075-15-2022-312 dated 20 April 2022).

Competing interest The authors have no competing interests to declare that are relevant to the content of this article.

References

Ahmed A, Younis M (2019) Acoustic beam characterization and selection for optimized underwater communication. Appl. Sci. 9(13): 2740. https://doi.org/10.3390/app9132740

Ahmad I, Rahman T, Zeb A, Khan I, Othman MTB, Hamam H (2022) Cooperative energy-efficient routing protocol for underwater wireless sensor networks. Sensors 22(18): 6945. https://doi.org/10.3390/s22186945

Ahmed SH, Lee S, Park J, Kim D, Rawat DB (2017) IDFR: Intelligent directional flooding-based routing protocols for underwater sensor networks. Proceedings of the 2017 14th IEEE Annual Consumer Communications Networking Conference (CCNC), Las Vegas, USA, 560-565. https://doi.org/10.1109/CCNC.2017.7983168

Akyildiz IF, Pompili D, Melodia T (2005) Underwater acoustic sensor networks: Research challenges. Ad Hoc Netw 3: 257-279. https://doi.org/10.1016/j.adhoc.2005.01.004

Alfajeer AA, Harous S (2022) A review of routing protocols for underwater wireless sensor networks. Proceedings of the 3rd International Conference on Distributed Sensing and Intelligent Systems (ICDSIS 2022), Sharjah, United Arab Emirates, 138-145. https://doi.org/10.1049/icp.2022.2428

Ali T, Jung LT, Faye I (2014) A reliable data flooding in underwater wireless sensor network. Proceedings of the First International Conference on Advanced Data and Information Engineering (DaEng-2013). Lecture Notes in Electrical Engineering 285: 499-511. https://doi.org/10.1007/978-981-4585-18-7_56

Aljughaiman A, Akanbi O, Aljaedi A, Chow E (2020) A survey on MAC protocol approaches for underwater wireless sensor networks. IEEE Sensors Journal 21(3): 3916-3932. https://doi.org/10.1109/JSEN.2020.3024995

Andreeva IB (1975) The physical basis of sound propagation in the ocean. Leningrad: Gidrometeoizdat. Aquatec Group Ltd. https://aquatecgroup.com

Arivudainambi D, Balaji S, Poorani TS (2017) Sensor deployment for target coverage in underwater wireless sensor network. Proceedings of the 2017 International Conference on Performance Evaluation and Modeling in Wired and Wireless Networks (PEMWN), Paris, 1-6. https://doi.org/10.23919/PEMWN.2017.8308032

Azam I, Majid A, Sajjad TK, Khan ZA, Qasim U, Javaid N (2016) Avoiding energy holes in underwater wireless sensor networks with balanced load distribution. Proceedings of the 10th International Conference on Complex, Intelligent, and Software Intensive Systems (CISIS), Fukuoka, 341-350. https://doi.org/10.1109/CISIS.2016.109

Basagni S, Petrioli C, Petroccia R, Stojanovic M (2012) Optimized packet size selection in underwater wireless sensor network communications. IEEE Journal of Oceanic Engineering 37(3): 321-337. https://doi.org/10.1109/JOE.2012.2197271

Bernard C, Bouvet PJ, Tomasi B (2022) Spread spectrum modulation with grassmannian constellations for mobile multiple access underwater acoustic channels. Sensors 22: 8518. https://doi.org/10.3390/s22218518

Bharany S, Sharma S, Alsharabi N, Eldin ET, Ghamry NA (2023) Energy-efficient clustering protocol for underwater wireless sensor networks using optimized glowworm swarm optimization. Front. Mar. Sci., Sec. Ocean Observation 10: 1117787. https://doi.org/10.3389/fmars.2023.1117787

Cai W, Zhang M (2016) 3D dubins curves based path programming for mobile sink in underwater sensor networks. Electron. Lett. 53(1): 48-50. https://doi.org/10.1049/el.2016.3836

Cao XL, Jiang WH, Tong F (2018) Time reversal MFSK acoustic communication in underwater channel with large multipath spread. Ocean Eng. 152: 203-209. https://doi.org/10.1016/j.oceaneng.2018.01.035

Casari P, Ardizzon F, Tomasin S (2022) Physical layer authentication in underwater acoustic networks with mobile devices. Proceedings of WUWNet'22, Boston, USA 4: 1-8. https://doi.org/10.1145/3567600.3567604

Chaaf A, Muthanna MSA, Muthanna A, Alhelaly S, Elgendy IA, Iliyasu AM, El-Latif AAA (2021) Energy-efficient relay-based void hole prevention and repair in clustered Multi-AUV underwater wireless sensor network. Security and Communication Networks, 9969605. https://doi.org/10.1155/2021/9969605

Chaudhary M, Goyal N, Benslimane A, Awasthi LK, Alwadain A, Singh A (2022) Underwater wireless sensor networks: enabling technologies for node deployment and data collection challenges. IEEE Internet of Things Journal 10(4): 3500-3524. https://doi.org/10.1177/1550132922112353310.1109/JIOT.2022.3218766

Chen H, Zhu Y, Zhang W, Wu K, Yuan F (2022) Underwater acoustic micromodem for underwater internet of things. Wireless Communications and Mobile Computing, 9148756. https://doi.org/10.1155/2022/9148756

Chen YS, Juang TY, Lin YW, Tsai IC (2010) A low propagation delay Multi-path routing protocol for underwater sensor networks. Journal of Internet Technology 11(2): 153-165. https://doi.org/10.6138/JIT.2010.11.2.03

Choudhary M, Goyal N (2021) Node deployment strategies in underwater wireless sensor network. Proceedings of the 2021 International Conference on Advance Computing and Innovative Technologies in Engineering (ICACITE), Greater Noida, India, 773-779. https://doi.org/10.1109/ICACITE51222.2021.9404617

Choudhary M, Goyal N (2022) Dynamic topology control algorithm for node deployment in mobile underwater wireless sensor networks. Concurrency and Computation Practice and Experience 34(15): e6942. https://doi.org/10.1002/cpe.6942

Climent S, Sanchez A, Capella JV, Meratnia N, Serrano JJ (2014) Underwater acoustic wireless sensor networks: advances and future trends in physical, MAC and routing layers. Sensors 14: 795-833. https://doi.org/10.3390/s140100795

Coutinho RWL, Boukerche A, Vieira LFM, Loureiro AAF (2018) Underwater wireless sensor networks: A new challenge for topology control-based systems. ACM Comput. Surv. 51(1): 1-36. https://doi.org/10.1145/3154834

Datta A, Dasgupta M (2023) Energy efficient topology control in Underwater Wireless Sensor Networks. Computers and Electrical Engineering 105: 108485. https://doi.org/10.1016/j.compeleceng.2022.108485

Davis A, Chang H (2012) Underwater wireless sensor networks. Proceedings of IEEE 2012 Oceans, Hampton Roads, USA, 1-5. https://doi.org/10.1109/OCEANS.2012.6405141

Di Valerio V, Petrioli C, Pescosolido L, Van der Shaar M (2015) A reinforcement learning-based data-link protocol for underwater acoustic communications. Proceedings of WUWNet 15(2): 1-5. https://doi.org/10.1145/2831296.2831338

Fattah S, Ahmedy I, Idris MYI, Gani A (2022) Hybrid multi-objective node deployment for energy-coverage problem in mobile underwater wireless sensor networks. International Journal of Distributed Sensor Networks 18(9): 155013292211235. https://doi.org/10.1177/15501329221123533

Fedorova TA, Ryzhov VA, Semenov NN, Sulaiman SA (2022) Optimization of an underwater wireless sensor network architecture with wave glider as a mobile gateway. Journal of Marine Science and Application 21: 179-196. https://doi.org/10.1007/s11804-022-00268-9

Fox-Kemper B, Johnson L, Qiao F (2022) Ocean near-surface layers. Ocean mixing ocean near-Surface layers. Environmental Science, 65-94. https://doi.org/10.1016/B978-0-12-821512-8.00011-6

Freitag L, Grund M, Singh S, Partan J, Koski P, Ball K (2005) The WHOI micro-modem: an acoustic communications and navigation system for multiple platforms. Proceedings of Oceans 2005 MTS/IEEE, Washington, USA, 2: 1086-1092. https://doi. org/10.1109/OCEANS.2005.1639901

Gazi F, Ahmed N, Misra S, Wei W (2022) Reinforcement learning-based MAC protocol for underwater multimedia sensor networks. CM Transactions on Sensor Networks 18(3): 1-25. https://doi.org/10.1145/3484201

Goyal N, Dave M, Verma AK (2019) Data aggregation in underwater wireless sensor network: recent approaches and issues. Journal of King Saud University-Computer and Information Sciences 31(3): 275-286. https://doi.org/10.1016/j.jksuci.2017.04.007

Guqhaiman AA, Akanbi O, AljaediA, Chow CE (2020) A survey on MAC protocol approaches for underwater wireless sensor networks. IEEE Sensors Journal 21(3): 3916-3932. https://doi.org/10.1109/JSEN.2020.3024995

Hao K, Ding Y, Li C, Wang B, Liu Y, Du X, Wang CQ (2021) An energy-effificient routing void repair method based on an autonomous underwater vehicle for UWSNs. IEEE Sensors Journal 21(4): 5502-5511. https://doi.org/10.1109/JSEN.2020.3030019

He C, Zhang Q, Yan Z, Li Q, Zhang L, Chen J, Qi Q (2017) Experimental demonstration of phase-coherent underwater acoustic communications using a compact array. Ocean Eng. 145: 207-214. https://doi.org/10.1016/j.oceaneng.2017.08.058

Hefeeda M, Ahmadi H (2007) Network connectivity under probabilistic communication models in wireless sensor networks. Proceedings of IEEE Internatonal Conf. Mobile Adhoc Sensor Syst., Pisa, Italy, 1-9. https://doi.org/10.1109/MOBHOC.2007.4428600

Heidemann J, Stojanovic M, Zorzi M (2012) Underwater sensor networks: applications, advances, and challenges. Philosophical Transactions of the Royal Society. A: Mathematical, Physical and Engineering Sciences 370: 158-175. https://doi.org/10.1098/rsta.2011.0214

Heinzelman WB, Chandrakasan AP, Balakrishnan H (2002) An application-specific protocol architecture for wireless microsensor networks. IEEE Trans. Wirel. Commun 1: 660-670. https://doi.org/10.1109/TWC.2002.804190

Hong Z, Pan X, Chen P, Su X, Wang N, Lu W (2018) A topology control with energy balance in underwater wireless sensor networks for IoT-based application. Sensors 18: 2306. https://doi.org/10.3390/s18072306

Hu Y, Hu K, Liu H, Wan X (2022) An energy-balanced head nodes selection scheme for underwater mobile sensor networks. EURASIP Journal on Wireless Communications and Networking 63: 1-21. https://doi.org/10.1186/s13638-022-02141-3

Hyder W, Nadeem A, Basit A, Rizwan K, Ahsan K, Mehmood N (2017) A review and classification of energy efficient MAC protocols for underwater wireless sensor network. Journal of Basic and Application Sciences 13: 63-70. https://doi.org/10.6000/1927-5129.2017.13.12

Isufi E, Dol H, Leus G (2016) Advanced flooding-based routing protocols for underwater sensor networks. EURASIP J. Adv. Signal Process 52: 1-12. https://doi.org/10.1186/s13634-016-0346-y

Jahanbakht M, Xiang W, Hanzo L, Azghadi MR (2021) Internet of underwater things and big marine data analytics-a comprehensive survey. IEEE Communication Surveys & Tutorials 23(2): 904-956. https://doi.org/10.1109/COMST.2021.3053118

Jawhar I, Mohamed N, Al-Jaroodi J, Zhang S (2019) An architecture for using autonomous underwater vehicles in wireless sensor networks for underwater pipeline monitoring. IEEE Trans. Ind. Inform. 15(3): 1329-1340. https://doi.org/10.1109/TII.2018.2848290

Jiang S (2018) State-of-the-art medium access control (MAC) protocols for underwater acoustic networks: A survey based on a MAC reference model. IEEE Communications Surveys & Tutorials 20(1): 96-131. https://doi.org/10.1109/COMST.2017.2768802

Jiang W, Yang X, Tong F, Yang Y, Zhou T (2022) A low-complexity underwater acoustic coherent communication system for small AUV. Remote Sens. 14: 3405. https://doi.org/10.3390/rs14143405

Jung LT, Abdullah AB (2011) Underwater wireless network energy efficiency and optimal data packet size. Proceedings of International Conference on Electrical, Control and Computer Engineering (INECCE), Kuantan, Malaysia, 178-182. https://doi.org/10.1109/INECCE.2011.5953871

Kampen AL (2021) Protocols for underwater wireless sensor networks-challenges and solutions. Proceedings of SENSORCOMM 2021: The Fifteenth International Conference on Sensor Technologies and Applications, Athens, Greece, 34-40

Kebkal A, Kebkal K, Komar M (2005) Data-link protocol for underwater acoustic networks. Proceedings of Europe Oceans 2005, Brest, France, 2. https://doi.org/10.1109/OCEANSE.2005. 1513225

Kebkal K, Mashoshin A, Morozs N (2019) Solutions for underwater communication and positioning network development. Gyroscopy and Navigation 10: 161-179. https://doi.org/10.1134/S2075108719030040

Khan ZA, Karim OA, Abbas S, Javaid N, Bin Zikria Y, Tariq U (2021) Q-learning based energy-efficient and void avoidance routing protocol for underwater acoustic sensor networks. Computer Networks 197: 108309. https://doi.org/10.1016/j.comnet.2021.108309

Khan ZU, Gang Q, Muhammad A, Muzzammil M, Khan SU, Affendi ME, Ali G, Ullah I, Khan J (2022) A comprehensive survey of energy-efficient MAC and routing protocols for underwater wireless sensor networks. Electronics 11(19): 3015. https://doi.org/10.3390/electronics11193015

Khasawneh AM, Kaiwartya O, Lloret J, Abuaddous HY, Abualigah L, Al-Shinwan M, Al-Khasawneh MA, Mahmoud M, Kharel R (2020) Green communication for underwater wireless sensor networks: Triangle metric based multi-layered routing protocol. Sensors 20: 7278. https://doi.org/10.3390/s20247278

Kulla E, Matsuo K, Barolli L (2022) MAC layer protocols for underwater acoustic sensor networks: A survey. In: Lecture Notes in Networks and Systems (LNNS), 496. https://doi.org/10.1007/978-3-031-08819-3_21

Lan H, Lv Y, Jin J, Li J, Sun D, Yang Z (2021) Acoustical observation with multiple wave gliders for internet of underwater things. IEEE Internet of Things Journal 8(4): 2814-2825. https://doi.org/10.1109/JIOT.2020.3020862

Li J, Tong F, Jiang W, Roy S (2022) Underwater acoustic modem with high precision ranging capability based on second-level cesium atomic clock. The International Archives of the Photogrammetry, Remote Sensing and Spatial Information Sciences, vol. XLVI-3/W1-2022-7th Intl. Conference on Ubiquitous Positioning, Indoor Navigation and Location-Based Services (UPINLBS 2022), Wuhan, China,18-19

Liu C, Zhao Z, Qu W, Qiu T, Sangaiah AK (2019) A distributed node deployment algorithm for underwater wireless sensor networks based on virtual forces. Journal of Systems Architecture 97: 9-19. https://doi.org/10.1016/j.sysarc.2019.01.010

Liu L, Liu Y, Zhang N (2014) A complex network approach to topology control problem in underwater acoustic sensor networks. IEEE Trans. Parallel Distrib. Syst. 25(12): 3046-3055. https://doi.org/10.1109/TPDS.2013.2295793

Liu X, Du X, Li M, Wang L, Li C (2021) A MAC protocol of concurrent scheduling based on spatial temporal uncertainty for underwater sensor networks. Hindawi Journal of Sensors, 5558078. https://doi.org/10.1155/2021/5558078

Lu Q, Liu F, Zhang Y, Jiang S (2017) Routing protocols for underwater acoustic sensor networks: A survey from an application perspective. In: Zak A (Eds.) Advances in Underwater Acoustics. IntechOpen, 144. http://dx.doi.org/10.5772/intechopen.68900

Lu Q, Shengming J (2016) A review of routing protocols of underwater acoustic sensor networks from application perspective. Proceedings of 2016 IEEE International Conference on Communication Systems (ICCS), Shenzhen, China, 1-6. https://doi.org/10.1109/ICCS.2016.7833633

Mani S, Duman TM, Hursky P (2008) Adaptive coding/modulation for shallow-water UWA communications. The Journal of the Acoustical Society of America 123(5): 3749. https://doi.org/10.1121/1.2935305

Margulis IM, Margulis MA (2005) Measurement of acoustic power in the study of cavitation processes. Acoistical Physics 51: 695-704. https://doi.org/10.1134/1.2130901

Menon VG, Prathap PJ (2016) Comparative analysis of opportunistic routing protocols for underwater acoustic sensor networks. Proceedings of 2016 International Conference on Emerging Technological Trends (ICETT), Kollam, India, 1-5. https://doi.org/10.1109/ICETT.2016.7873733

Mhemed R, Phillips W, Comeau F, Aslam N (2022) Void avoiding opportunistic routing protocols for underwater wireless sensor networks: A survey. Sensors 22: 9525. https://doi.org/10.3390/s22239525

Miguel AJ (2003) Construction and testing of low-noise hydrophones. PhD thesis, Naval Postgraduate School, Monterey, California, 66. https://core.ac.uk/download/pdf/36699935.pdf

Nam H (2018) Data-gathering protocol-based AUV path-planning for long-duration cooperation in underwater acoustic sensor networks. IEEE Sens. J. 18(21): 8902-8912. https://doi.org/10.1109/JSEN.2018.2866837

Ovchinnikov KD, Ryzhov VA, Sinishin AA, Kozhemyakin IV (2020) Experimental study of running characteristics of wave glider. Proceedings of XV All-Russian Scientific and Practical Conference "Advanced systems and control problems", Southern Federal University Press, 91-97

Pan X, Jiang J, Li S, Ding Z, Pan C, Gong X (2018) Coherent and noncoherent joint processing of sonar for detection of small targets in shallow water. Sensors 8(4): 1154. https://doi.org/10.3390/s18041154

Pompili D, Melodia T, Akyildiz (2010) Distributed routing algorithms for underwater acoustic sensor networks. IEEE Trans. Wireless Commun. 9(9): 2934-2944. https://doi.org/10.1109/TWC.2010.070910.100145

Rahman MA, Lee Y, Koo I (2017) EECOR: an energy efficient cooperative opportunistic routing protocol for underwater acoustic sensor networks. IEEE Access 5: 14119-14132. https://doi.org/10.1109/ACCESS.2017.2730233

Rahman T, Ahmad I, Zeb A, Khan I, Ali G, Affendi M (2023) Performance evaluation of routing protocols for underwater wireless sensor networks. J. Mar. Sci. Eng. 11(38). https://doi.org/10.3390/jmse11010038

Rajeswari A, Duraipandian N, Shanker NR, Samuel BE (2020) Improving packet delivery performance in water column variations through LOCAN in underwater acoustic sensor network. Hindawi Journal of Sensors 7960654: 16. https://doi.org/10.1155/2020/7960654

Schmidt JH, Schmidt AM, Kochanska I (2019) Performance of coherent modulation scheme used in acoustic underwater communication system. Vibrations in Physical Systems 30: 2019135. http://yadda.icm.edu.pl/baztech/element/bwmeta1.element.baztech-268e16e1-d911-4ec4-9648-82e4032b674d

Scussel KF, Rice JA, Merriam S (1997) A new MFSK acoustic modem for operation in adverse underwater channels. Proceedings of Oceans 97. MTS/IEEE Conference, Halifax, Canada. https://doi.org/10.1109/OCEANS.1997.634370

Shahapur SS, Khanai R (2015) Underwater sensor network at physical, data link and network layer - a survey. Proceedings of 2015 International Conference on Communications and Signal Processing (ICCSP), Melmaruvathur, India. https://doi.org/10.1109/ICCSP.2015.7322753

Sharma A, Bindal AB (2014) Deployment issues in underwater wireless sensor networks: A survey report. International Journal of Computer Science and Technology 5(2): 451-454. https://www.researchgate.net/publication/273443079_Deployment_Issues_in_Underwater_Wireless_Sensor_Networks_A_Survey_Report/link/5e5f86de4585152ce8053ea9/download

Sheeja R, Iqbal MM, Sivasankar C (2023) Multi-objective-derived energy efficient routing in wireless sensor network using adaptive black hole-tuna swarm optimization strategy. Ad Hoc Networks 144: 103140. https://doi.org/10.1016/j.adhoc.2023.103140

Shental O, Shental N, Shamai S (2005) On the achievable information rates of finite-State input two-dimensional channels with memory. Proceedings of IEEE Int. Symp. Inform. Theory (ISIT), Adelaide, Australia, 2354-2358. https://doi.org/10.1109/ISIT.2005.1523769

Sherlock B, Morozs N, Neasham J, Mitchell P (2022) Ultra-low cost and ultra-low-power, miniature acoustic modems using multipath tolerant spread spectrum techniques. Electronics 11: 1446. https://doi.org/10.3390/electronics11091446

Shovon II, Shin S (2022) Survey on multi-path routing protocols of underwater wireless sensor networks: Advancement and applications. Electronics 11: 3467. https://doi.org/10.3390/electronics11213467

Singh H (2020) Sifting sound interactive extraction, exploration, and expressive recombination of large and heterogeneous audio collections. Master thesis, Massachusetts Institute of Technology, School of Architecture and Planning, Program in Media Arts and Sciences, 1-115

Songzuo L, Iqbal B, Khan IU, Ahmed N, Qiao G, Zhou F (2021) Full duplex physical and MAC layer-based underwater wireless communication systems and protocols: Opportunities, challenges, and future directions. J. Mar. Sci. Eng. 9: 468. https://doi.org/10.3390/jmse9050468

Stojanovic M (2005) Optimization of a data link protocol for an underwater acoustic channel. Proceedings of Europe Oceans, Brest, France, 2. https://doi.org/10.1109/OCEANSE.2005.1511686

Stojanovic M (2007) On the relationship between capacity and distance in an underwater acoustic communication channel. Proceedings of the First Workshop on Underwater Networks, WUWNET 2006, Los Angeles, USA, 41-47. https://doi.org/10.1145/1161039.1161049

Sutagundar AV, Halakarnimath BS, Bhajantri LB, Nalini N (2022) A novel approach of topology control in underwater sensor networks. Proceedings of 2022 IEEE 2nd Mysore Sub Section International Conference (MysuruCon), Mysuru, India, 1-5. https://doi.org/10.1109/MysuruCon55714.2022.9972400

Tan YJ, Wu J (2004) Network structure entropy and its application to to scale-free networks. Syst. Eng. Theory Pract. 24(6): 1-3. https://doi.org/10.12011/1000-6788(2004)6-1

Tang MQ, Sheng JW, Sun SY (2023) A coverage optimization algorithm for underwater acoustic sensor networks based on Dijkstra method. IEEE/CAA J. Autom. Sinica, 1769-1771. DOI: 10.1109/JAS.2023.123279

Thorp WH (1965) Deep sound attenuation in the sub and low kilocycle per-second Range. J. Acoust. Soc. Am. 38: 648-654. https://doi.org/10.1121/1.1909768

Tiwari KK, Singh S (2023) Energy-optimized cluster head selection based on enhanced remora optimization algorithm in underwater wireless sensor network. International Journal of Communication Systems 36 (15): e5560. https://doi.org/10.1002/dac.5560

Tokmachev DA, Chensky AG, Zolotarev NS, Poletaev AS (2021) Modelling of a hydroacoustic modem for underwater communications. J. Phys.: Conf. Ser. 1728: 012021. https://doi.org/10.1088/1742-6596/1728/1/012021

Touzen A (2020) Energy efficient broadcast protocol for Underwater Wireless Sensor Networks. CCF Transactions on Networking 3: 1-10. https://doi.org/10.1007/s42045-021-00049-y

Ulvestad A (2018) A brief review of current lithium ion battery technology and potential solid state battery technologies. Materials Science Applied Physics 18(3). https://arxiv.org/abs/1803.04317

Urick RJ (2013) Principles of underwater sound. Third editiona, Peninsula Publishing, 423. https://pdfgoes.com/download/1707527-Principle%20Of%20Underwater%20Sound%20Urick.pdf

Venkateswara Rao M, Malladi S (2021) Improving packet delivery ratio in wireless sensor network with multi factor strategies. International Journal of Advanced Computer Science and Applications 12(5): 627-634. https://doi.org/10.14569/IJACSA.2021.0120575

Vhatkar S, Mehta S, Atique M (2015) Performance evaluation and QoS analysis of BCDCP and CBCB routing protocols in wireless sensor networks. Communications on Applied Electronics (CAE), Foundation of Computer Science FCS 3(4). https://doi.org/10.5120/cae2015651948

Vijay MM, Sunil J, Vincy VGAG, IjazKhan M, Abdullaev ShSh, Eldin SM, Govindan V, Ahmad H, Askar S (2023) Underwater wireless sensor network-based multihop data transmission using hybrid cat cheetah optimization algorithm. Sci. Rep. 13: 10810. https://doi.org/10.1038/s41598-023-37952-x

Wang D, You M, Xu W, Wang L (2022) Subcarrier index modulation aided Non-Coherent chaotic communication system for underwater acoustic communications. Proceedings of Wireless Algorithms, Systems, and Applications: 17th International Conference, WASA 2022, Dalian, China, 621-634. https://doi.org/10.1007/978-3-031-19214-2_52

Wang J, Ma L, Chen W (2017) Design of underwater acoustic sensor communication systems based on software-defined networks in big data. International Journal of Distributed Sensor Networks 13(7): 15501477177. https://doi.org/10.1177/1550147717719672

Xu Y, Zhang H, Pang Z, Kang Y, Su Y (2022) Design and implementation of a transport protocol with network coding for delay tolerant underwater acoustic sensor networks. OCEANS 2022, Chennai, India, 21-24. https://doi.org/10.1109/OCEANSChennai45887.2022.9775134

Yang Q, Su Y, Jin Z, Yao G (2015) EFPC: An environmentally friendly power control scheme for underwater sensor networks. Sensors 15(11): 29107-29128. https://doi.org/10.3390/s151129107

Yigit M, Yildiz HU, Kurt S, Tavli B, Gungor VC (2018) A survey on packet size optimization for terrestrial, underwater, underground, and body area sensor networks. International Journal of Communication Systems 31(11): e3572. https://doi.org/10.1002/dac.3572

Yildiz HU, Gungor VC, Tavli B (2018). Packet size optimization for lifespan maximization in underwater acoustic sensor networks. IEEE Transactions on Industrial Informatics 15(2): 719-729. https://ieeexplore.ieee.org/document/8368321

Zhang AM, Li SM, Cui P, Li S, Lui YL (2023) A unified theory for bubble dynamics. Physics of Fluids 35(3): 033323. https://doi.org/10.1063/5.0145415

Zia MYI, Poncela J, Otero P (2021) State-of-the-art underwater acoustic communication modems: classifications, analyses and design challenges. Wireless Personal Communications 116:1325-1360. https://doi.org/10.1007/s11277-020-07431-x

Zorzi M, Casari P, Baldo N, Harris AF (2008) Energy-efficient routing schemes for underwater acoustic networks. IEEE J. Sel. Areas Commun 26(9): 1754-1766. https://doi.org/10.1109/JSAC.2008.081214